Spring 5-2014

Critical Speed Analysis of Railcars and Wheelsets on Curved and Straight Track

Joanna Charlotte Moody
Bates College

Critical Speed Analysis of Railcars and Wheelsets on Curved and Straight Track

An Honors Thesis

Presented to the Department of Physics and Astronomy

Bates College

in partial fulfillment of the requirements for the

Degree of Bachelor of Science

by

Joanna Moody

Lewiston, Maine

April 1, 2014

Acknowledgments

I have had to overcome many stressful obstacles along the way toward the culmination of this thesis; however, I was fortunate enough not to have to tackle these obstacles alone. This thesis would not be all that it is had I not had the support of many people, including my professors, both within and outside the physics department, my friends, and my family. In particular, I would like to thank my thesis advisor, Nathan Lundblad, for allowing me to pursue my passion and for being willing to advise a thesis outside of his comfort zone. He has not only been an indispensable resource to me in composing this thesis, but has also served as a mentor for me since my first year at Bates. I would like to thank Lucas Wilson-Spiro for nursing me back to health through my concussion and for reminding me that I can overcome whatever problems that I may face. A thank you also to Graham Oxman, who pushed me to never give up and reminded me that it was okay to seek help when I was struggling the most. To my family - mother, father, older and younger sisters - thank you each for supporting me in your own way.

Lastly, I would like to take the time to thank anyone who reads some or all of this thesis. Being able to share my work and add even a small contribution to collective scholarship is the ultimate reward for completing this project. I hope you enjoy.

Contents

List of Figures

List of Tables

Introduction

Railroad has provided the safest form of transport for more than 150 years and is one of the oldest forms of land transportation still in use today. Trains, with tracks and self-steering wheels, are fundamentally safer than vehicles that are almost completely controlled by drivers or pilots prone to human error. Accident statistics offer real insight into the differences in safety between the main modes of human transportation. In the United States there is an auto-accident fatality in every 100 million passenger miles [8]. Whereas, there is only one passenger death for every three billion miles traveled by rail [9]. To frame the statistics another way, passengers in trains were 19 times safer than passengers in cars and 6 times safer than passengers in buses in a recent 5-year period. In fact, passenger train fatalities are so rare that one bad accident drastically alters the statistics. For example, eliminating the single worst U.S. passenger train accident in the twenty-first century, passengers in trains are up to 45 times safer than those in cars [8]. Although some statistics may indicate that air travel has surpassed rail in safety, these comparisons are misguided because they look not at the number of passenger journeys but at the total distances traveled [9]. This means that a single transatlantic flight and return counts the same as three months of commuting thirty miles a day by rail. The railroad industry is proud of this safety record and looks to new innovation and network upgrades only if they meet strict safety requirements.

Growing world populations and economies are putting new pressures on this well-established transport system. To meet rising demand, railroad managers and engineers are looking to increase traffic flow, either through increased speed or more numerous, longer trains. However, in the United States existing infrastructure limits the options available for improving efficiency while maintaining current levels of safety. Although rail transport is safe, railroad derailment remains one of the most pervasive types of rail accidents. Railroads are so safe that most people do not consider the intricacy, and also imperfection, of the dynamic behavior of the railcar and wheelset down the track. Often the same, age-old systems that give rise to vehicle stability and steering can, under abnormal or extreme conditions, cause instability or derailment. Primarily three categories of defects can cause a derailment: rail and track factors, equipment and loading factors, and operational factors [16]. Therefore

this thesis looks to apply a fundamental understanding of the physical system of the railcar and wheelset to help explain how changes in rail and wheelset geometries as well as railcar loading can affect the stability of the railcar and train on curved and straight sections of flat track.

Railroad transport relies on adhesive traction between wheel and rail. Adhesion, or the tendency of dissimilar surfaces to cling to one another, is a frictional phenomenon that allows the circular steel wheel to roll, as opposed to slide, along the track. A railway train running along a track is one of the most complex dynamic systems in engineering and its operation has two main features: motion in a string of vehicles, and guidance by the track [26]. In a complete model of the dynamics of a railway vehicle, the vehicle is assembled from wheelsets, car bodies, and intermediate structures that are all flexible and connected by components such as springs and dampers. Each major component has six rigid body degrees of freedom plus additional degrees of freedom representing distortion and vibration [7]. In addition, the vehicle runs on a complex track structure with elastic and dissipative properties. The track and wheelset have points of contact in a moving interface and therefore interactions between wheel and rail depend on relative motion.

This entire physical system is so complex that often analytic methods fail and engineers are left only with numerical simulation. However, simpler models that describe the mechanics of various subsystems of the larger physical system can be solved exactly and used to develop a basis for a greater physical understanding and to explore new vehicle concepts and component designs. Within this complex physical system, it is the guidance of the train by the interaction between fixed wheelset and track that is one of the most interesting and unique features of railways. Unlike with other forms of transportation, guidance or direction are the responsibility of a built-in rail infrastructure as opposed to a driver. In addition to being a unique feature of railroads, this built-in guidance and stability system also means that most railcar and train behavior is described by the physical and mechanical constraints of the system. Therefore, understanding the fundamental motions of a railcar or wheelset on rail is vital to any analysis of the safety and riding comfort of railroad cars on either curved or straight track.

When modeling the dynamics (and stability) of the railcar or wheelset, there are a number of assumptions that can simplify the problem. First, assuming that the vehicle has a longitudinal plane of symmetry parallel to the direction of motion on straight track makes it possible, under certain conditions, to separate equations of motion that are symmetric with respect to the plane of symmetry from those that are anti-symmetric. Second, these models need not consider variations in longitudinal motion, so that the vehicle moves at a constant speed forward. And finally, the flexibility of components can be neglected since

in most cases the motions of interest are at low frequencies [26]. A kinematic description deals mainly with the geometry of motion and the component-wise sum of the many forces causing it.

Due to these assumptions, any equations derived from this kinematic analysis are necessarily approximations. Therefore this thesis is not meant to give exact values for track speed limits on curved and straight track; there are higher-level computer simulations that can give more exact answers. Instead, this thesis is meant to apply fundamental physical principles to a subject otherwise rooted in complex engineering mechanics. In this way I hope to help a reader less familiar with the infrastructures of the industry understand the design choices of railroad management and engineers. I first present the kinematic analysis of a railcar and wheelset on curved track in order to derive expressions for maximum speed given geometric constraints of the wheelset (see Appendix A), track, and railcar. I discuss how these design parameters and geometries can be manipulated by the industry to increase speeds and improve the flow of traffic along existing curved sections. A similar analysis follows for straight track. Here I motivate equations of periodic motion and also derive equations of critical speed. The final chapter again explores how changes in the parameters of these motion and speed equations can inform track design.

We will ultimately see that optimizing both curved and straight track design for improved flow of traffic is difficult for shared corridors, where the rails are used by freight and passenger traffic. From the kinematic approximations we can clearly see that stabilizing the dynamics of heavy, long, heterogeneous, and slow trains suggests solutions that restrict the running speeds of faster, lighter, and shorter passenger trains. Understanding the fundamental physics behind these separate dynamic issues can suggest a compromise that solves the shared-corridor problem faced by the railroad industry today, especially within the United States.

Chapter 1

Kinematic Analysis of the Railcar and Wheelset on Curved Track

This chapter explores how the forces on a railcar during curving can introduce both maximum and minimum speeds on curved sections of track. Any kinematic analysis of the wheelset and railcar necessarily begins with a description of the geometry of a wheelset, which we have set aside in Appendix A. The following sections show how particular features of the railroad wheelset, namely the coning of the tread and flange, affect the dynamics of the railcar on curved track.

All figures in this chapter are drawn as if the train is going around a left-hand curve.

1.1 Wheelset Geometry and the Role of the Conicity

In curving situations, the conicity of the wheel treads serves a similar function to the differential in an automobile [8]. In an automobile, the differential is necessary when the vehicle turns, because it allows the driving roadwheels to rotate at different speeds. This allows the wheel on the outside of the turning curve to roll faster (at a higher angular velocity) than the other, allowing it to traverse the greater distance. Unlike in an automobile, whose

differential allows the wheels to spin at different speeds, in a railcar the two wheels are fixed to a common axle and therefore must rotate at the same speed. In this case, it is the conicity that allows the wheel on the outside of the turn to move faster and cover the longer distance. On a gentle curve, the coned wheels maintain pure rolling motion by moving laterally outward and adopting a radial position. In this way, the wheel on the outside of the curve runs on a larger radius (and therefore circumference) and can travel the greater distance at the common angular speed; whereas the wheel on the inside of the curve rolls on its smaller radius and travels the smaller distance.

So a rigid wheelset with coned wheels maintains pure rolling motion in a gentle curve, without flange contact, if it moves laterally outward a distance y from the center of the track and adopts a radial position as shown in Figure 1.1.

Figure 1.1: Geometry of a coned wheelset on a gentle curve.

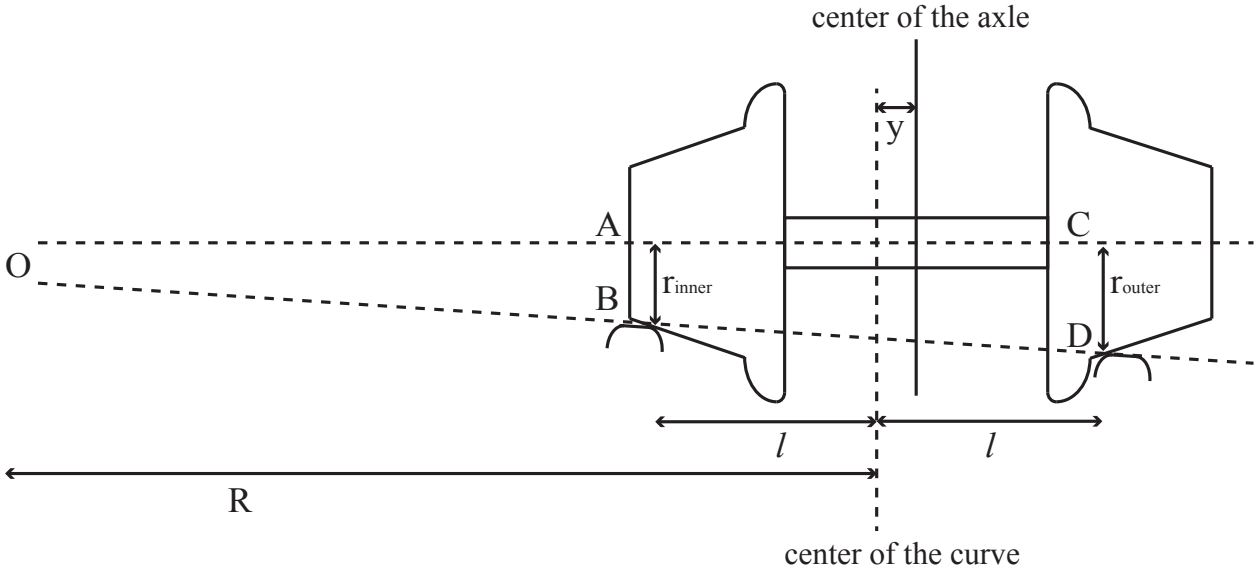

Following [26], we construct two rays from the origin of the curve, O. The first passes through the contact point of the inner wheel and rail, B, and the contact point of the outer wheel and rail, D. The second ray lies along the central axle axis, connecting the origin of the curve with the center of the inner wheel, A, and the center of the outer wheel, C. These two rays form an angle at the center of the curve and give rise to similar triangles AOB and COD. Using properties of similar triangles, we can write the relation:

$$\frac{r_{\text{inner}}}{R-l} = \frac{r_{\text{outer}}}{R+l}$$

where R is the radius of the curve, $2l$ is the track width or gauge (the lateral distance between

the points of contact of the wheels with the rails), r_{inner} is the radius of the wheel on the inside of the curve at the point of contact with the rail and r_{outer} is similarly the radius of the wheel on the outside of the curve at the point of contact with the rail. If we define the normal running radius, r to be the radius of both wheels when the wheelset is centered on the track, then we can rewrite r_{inner} and r_{outer} in terms of the conicity of the wheelset, α, and the lateral displacement of the wheelset, y.

$$r_{\text{inner}} = r - \alpha y$$
$$r_{\text{outer}} = r + \alpha y$$

By substituting these expressions for r_{inner} and r_{outer} into the similar triangles relation, we can solve for the lateral displacement y in terms of physical parameters of the wheel rail system: the tread conicity, α, normal wheel radius r, track gauge, $2l$, and radius of curvature, R:

$$\begin{aligned}
\frac{r - \alpha y}{R - l} &= \frac{r + \alpha y}{R + l} \\
(r - \alpha y)(R + l) &= (r + \alpha y)(R - l) \\
rR + l - \alpha yR - \alpha yl &= rR - rl + \alpha yR - \alpha yl \\
rl - \alpha yR &= -rl + \alpha yR \\
2rl &= 2\alpha yR \\
y &= \frac{rl}{R\alpha}
\end{aligned} \tag{1.1}$$

This equation (1.1) for the lateral displacement of a wheelset on a curve or radius R was first derived in 1855 by Redtenbacher [23]. Application of Redtenbacher's formula shows that a wheelset will only be able to move outwards to achieve pure rolling if either the radius of curvature or the flangeway clearance is sufficiently large. These geometric results ignore the forces causing the motion. These may be analyzed using the concept of non-linear creep that arises from the elastic distortion of the wheel and rail at the region of contact. This more intricate model employs the study of contact mechanics, which is beyond the scope of this work. So it is enough to know that, in practice, a wheelset can only roll around moderate curves without flange contact and a more realistic consideration of curving requires the analysis of the forces acting between the vehicle and the track.

1.2 Railcar Overturning and the Role of the Flange

According to Newton's Laws of Motion, a body in motion tends to stay in motion and a body at rest tends to stay at rest. The property of an object that resists changes in motion is called inertia. When a body accelerates, or changes velocity, that acceleration is accompanied by a force according to the equation $\vec{F} = m\vec{a}$, where the mass of the object m is its weight W divided by the gravitational acceleration constant, g. We tend to think of acceleration as being a change in speed; but since velocity is a vector, any change of velocity - be it a change in the magnitude (speed) or in the direction - requires a force. For instance, in circular motion at constant speed, there is an acceleration radially inward toward the center of rotation due to the changing direction of the tangential velocity. It is this centripetal acceleration (and accompanying force) that keeps the object moving in a circular path. However, the objects inertia resists this change and so always acts in the opposite direction of the acceleration, or in this case radially outward from the center of the circle.

For a railcar and attached wheelset going around a curve, it is the train's inertia that causes instability and guidance problems such as tipping or derailment. In stable curving, lateral forces between the wheels and the rail provide a centripetal acceleration equal to the square tangential velocity of the train down the track, V^2, divided by the radius of the curve, R.

$$a_c = V^2 \frac{1}{R}$$

The centripetal, or 'center-seeking,' force associated with this acceleration keeps the train in a circular, or curved path; however, the train's inertia acts in the opposite direction of this acceleration. Since the resistance from inertia has the same units as a force, it is commonly (and erroneously) referred to as the centrifugal force. Often these 'fictitious forces' arise from a difference in reference frames. From the viewpoint or reference frame of someone on the ground beside the track, there appears to be no force acting outward on the railcar. However, from the rotating reference frame of the railcar itself, the car's inertia resists the circular motion and the railcar experiences a push or pull similar to a force. In other words, the centrifugal force is simply the train's inertial resistance to the centripetal acceleration around a curve and can be calculated using $\vec{F} = m\vec{a}$. For a locomotive traveling at a forward speed V on a flat curve of radius R, the centrifugal inertial loading, as we will more aptly call it, is given by

$$F_{\text{inertia}} = ma = \left(\frac{W}{g}\right)\left(V^2 \frac{1}{R}\right)$$

Lateral forces between the wheels and the rail must react against the centrifugal inertial loading to keep the train on the tracks. If the centrifugal inertial loading is excessive, the

locomotive begins to tip. The flange of the wheel catches on the rail and the locomotive starts to rotate. In fact, this is why the flanges are on the inside of the wheels. In sharp curves, if the flange is on the inside, then the lateral force applied by the rail to the leading wheelset is applied to the outer wheel and will be combined with an enhanced vertical load, diminishing the risk of derailment. If the flanges were instead on the outside, the slightest bit of wheel lift would slide the locomotive off the tracks. Put another way, with outside flanges the lateral force applied by the rail is applied to the inner wheel, which has a reduced vertical load and thus runs the risk of derailment (see Figures 1.2 and 1.4).

1.2.1 On a Flat Curve

On a flat curve the centrifugal inertial loading is trying to tip the locomotive clockwise about the pivot point (the bottom of the right wheel). This rotation is resisted by the weight of the locomotive (also acting through its center of gravity), which tries to rotate the locomotive counterclockwise.

Figure 1.2: Railcar force diagram on a flat curve

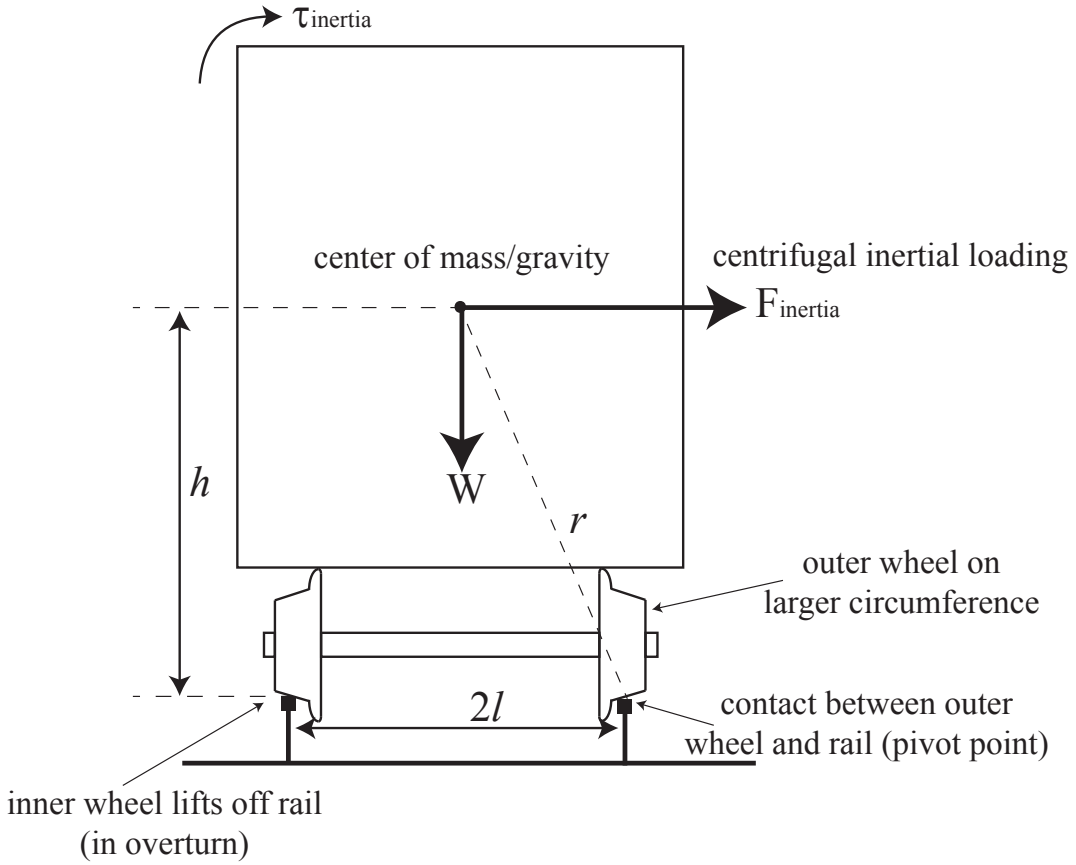

The locomotive's weight and inertial load both exert a torque. The inertial load tries to rotate the locomotive with a clockwise torque equal to $\vec{\tau}_{\text{inertia}} = \vec{F}_{\text{inertia}} \times \vec{r}$, where $\vec{r}$ is the vector pointing from the center of mass to the pivot point. For a railcar with center of mass at a height h above the top of the rails and located at the center of the gauge (a horizontal distance l from either rail), the vector cross product is equal to:

$$\tau_{\text{inertia}} = F_{\text{inertia}} r \sin(\beta) = \left(\frac{W}{g}\right)\left(V^2 \frac{1}{R}\right) h$$

The torque from the locomotive's weight, transferred between the outside wheel and rail via adhesion, tries to resist the overturning torque from the centrifugal inertial loading. The torque from the locomotive's weight is given by

$$\tau_{\text{weight}} = W r \sin(90^\circ - \beta) = W l$$

Tipping will occur when the torque from the inertial load is slightly larger than the torque from the locomotive's weight resisting the overturning torque. Since the centrifugal inertial loading depends on the speed of the locomotive, there is a critical speed at which, all geometries of the curve held constant, the overturning and resisting torques are equal. So setting $\tau_{\text{inertia}} = \tau_{\text{weight}}$ we can solve for this critical speed,

$$\begin{aligned} \left(\frac{W}{g}\right)\left(V^2 \frac{1}{R}\right) h &= W l \\ \left(V^2 \frac{1}{R}\right) &= \frac{lg}{h} \\ V_{max} &= \sqrt{\frac{gRl}{h}} \end{aligned} \tag{1.2}$$

In 1974, a Pennsylvania Railroad passenger train with 2 steam locomotives and 14 cars descended a steep 1.73% grade when it overturned on a sharp 8.5-degree flat curve, with a 675-foot radius, known as Bennington Curve. The speed limit downhill was 35 mph and 30 mph on the curve [5]. However, the area was infamous for its mountainous changes in incline and its winding curves, making it hard to precisely control speed and braking [17]. The train, called The Red Arrow, jumped the tracks killing twenty-four onboard and critically injuring scores of other passengers. The locomotives at the head of the train plunged down a 92-foot embankment with 5 cars attached and another 5 of the 14 cars derailed, making it one of the deadliest train crashes in American History (see Figure 1.3)[1].

[1]Photo courtesy of http://www.billspennsyphotos.com/apps/photos/album?albumid=8726232

Figure 1.3: The crash of Pennsylvania Railroad's Red Arrow on Bennington Curve, 1947.

The investigators concluded that excess speed caused the train to overturn on the curve. The overturning speed was calculated to be 65 mph [5]. This Pennsylvania Railroad train's lead locomotive had a center of gravity $h = 80$ inches above the rail and was running on normal gauge with $2l = 56.6$ inches. From Equation (1.2) for the critical speed of the onset of overturning, or the maximum safe speed for a flat curve, we find that the locomotive is just starting to overturn at a speed of 60 mph. We see that even our rough estimation of the critical speed from kinematic analysis explains why the train overturned at the speed of 65 mph, 5 mph over the maximum speed for a flat curve.

1.2.2 On a Superelevated Curve

The 1947 accident occurred on a flat curve, at a time when old infrastructure had yet to be upgraded to allow for faster speeds and higher traffic flows. In modern industrial practice, many tracks are designed so that rails are not flat on curves. Instead, the curve is banked so that the outside rail on a curve is elevated higher than the inside rail. This superelevation (or crosslevel in the US) is usually characterized by the height difference between the tops of the rails, but can also be measured in terms of angle or cant. The relationship between

the cant angle and superelevation height is dictated by the rail gauge according to simple right-triangle geometry (see Figure 1.5):

$$\sin\theta = \frac{s}{2l} \tag{1.3}$$

A raised outside rail rotates the train toward the inside of the curve and helps fight off the overturning rotation toward the outside of the curve caused by the centrifugal inertial loading (see Figure 1.4). Since some of the inertial torque is counteracted by the weight, the railcar can traverse the curve at a higher speed before overturning. In addition to allowing trains to travel through turns at higher maximum speeds, superelevation also helps keep the wheel flanges from pressing the rails, minimizing friction and wear.

Figure 1.4: Railcar force diagram on a superelevated curve.

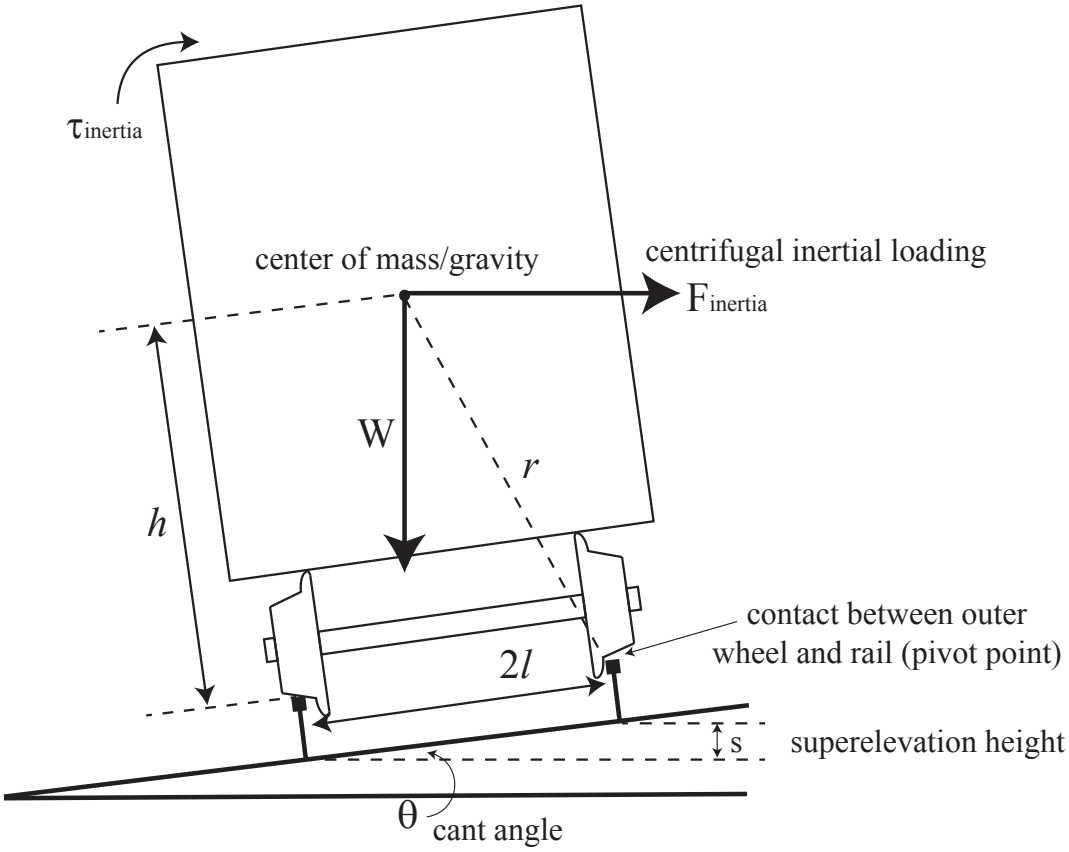

With a superelevated track, the torque due to the inertial loading still acts around the pivot of the contact point between the outside wheel and the rail. However, the angle between the inertial loading force and the pivot vector, $\vec{r}$, has been effectively reduced by the superelevation angle or cant angle, θ, as the car tilts in relation to the center of the

curve.

Figure 1.5: Geometry of the forces and torque arm for a railcar on a slightly superelevated curve.

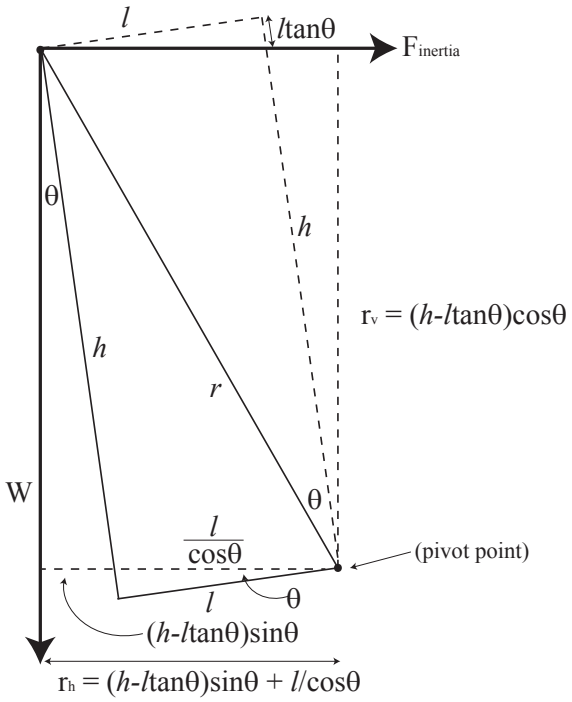

Given the geometry between the forces on the railcar and the torque arm from the center of the railcar mass to the outside wheel contact point (see Figure 1.5), we can find that the vertical distance between the pivot point and the inertial loading force is $r_v = (h - l\tan\theta)\cos\theta$. So the torque from the inertial loading, $\vec{\tau}_{\text{inertia}} = \vec{F}_{\text{inertia}} \times \vec{r}$, is given by the expression:

$$\begin{aligned}
\vec{\tau}_{\text{inertia}} &= F_{\text{inertia}} r_v \\
&= F_{\text{inertia}} \left[(h - l\tan\theta)\cos\theta\right] \\
&= F_{\text{inertia}} \left[h\cos\theta - l\sin\theta\right] \\
&= \left(\frac{W}{g}\right)\left(V^2\frac{1}{R}\right)\left[h\cos\theta - l\sin\theta\right]
\end{aligned}$$

Similarly, we can find the horizontal distance between the pivot point and the weight force vector in terms of l, h, and θ: $r_h = (h - l\tan\theta)\sin\theta + \frac{l}{\cos\theta}$. With this we find that the

torque due to the weight on a superelevated curve, $\vec{\tau}_{\text{weight}} = \vec{W} \times \vec{r}$ is given by:

$$\begin{aligned}
\vec{\tau}_{\text{weight}} &= W\left[(h - l\tan\theta)\sin\theta + \frac{l}{\cos\theta}\right] \\
&= W\left[h\sin\theta - l\left(\frac{\sin^2\theta}{\cos\theta}\right) + \frac{l}{\cos\theta}\right] \\
&= W\left[h\sin\theta - \frac{l}{\cos\theta}(\sin^2\theta - 1)\right] \\
&= W\left[h\sin\theta - \frac{l}{\cos\theta}(-\cos^2\theta)\right] \\
&= W\left[h\sin\theta + l\cos\theta\right]
\end{aligned}$$

Just as in the flat curve situation, the maximum or critical speed is where the torque toward the inside of the curve from the weight exactly counteracts the torque toward the outside of the curve from the inertial loading. So to find an expression for the maximum speed, we set τ_{inertia} equal to τ_{weight}:

$$\begin{aligned}
\left(\frac{W}{g}\right)\left(V^2\frac{1}{R}\right)\left[h\cos\theta - l\sin\theta\right] &= W\left[h\sin\theta + l\cos\theta\right] \\
\left(V^2\frac{1}{Rg}\right) &= \frac{\left[h\sin\theta + l\cos\theta\right]}{\left[h\cos\theta - l\sin\theta\right]} \\
V_{max} &= \sqrt{\frac{Rg[h\sin\theta + l\cos\theta]}{h\cos\theta - l\sin\theta}} \qquad (1.4)
\end{aligned}$$

It is important to note that when the cant angle θ equals zero (when there is no bank), the maximum speed on the superelevated curve, given by Equation (1.4), reduces to the maximum speed on a flat curve, given by Equation (1.2). Furthermore, we can show that, given the nonzero car and rail dimensions h and $2l$, this maximum speed for a banked curve is indeed always greater than the maximum speed for a flat curve. We find that the inequality $V_{\text{max elevated}} > V_{\text{max flat}}$ simplifies to a true statement:

$$\begin{aligned}
\sqrt{\frac{Rg[h\sin\theta + l\cos\theta]}{h\cos\theta - l\sin\theta}} &> \sqrt{\frac{lgR}{h}} \\
\frac{\left[h\sin\theta + l\cos\theta\right]}{h\cos\theta - l\sin\theta} &> \frac{l}{h} \\
h^2\sin\theta + hl\cos\theta &> hl\cos\theta - l^2\sin\theta \\
h^2 &> -l^2
\end{aligned}$$

The truth of this identity is obvious since positive numbers are always greater than negative

numbers. Thus we can conclude that our formula for $V_{\max \text{ elevated}}$ indeed gives us a speed greater than $V_{\max \text{ flat}}$ for any cant angle. Practically speaking, this means that railroad companies can bank curves to allow their trains to move faster along the track. This is desirable as it allows more efficient traffic flow along rail corridors.

Returning to the 1947 Pennsylvania Railroad derailment, investigators at the time concluded that the locomotive would have safely traversed the curve at its approach speed of 65 mph had the curve been superelevated to a height of 3.5 inches [5]. Converting this superelevation height to a cant angle using Equation (1.3), we get $\theta = 0.0619$ rad or $3.55°$. We can confirm that the Pennsylvania Railroad locomotive would not have overturned a curve banked at this angle because Equation (1.4) yields a maximum safe speed of over 70 mph, 5 mph above the locomotive's approach speed (given $R = 675$ ft, $2l = 56.6$ in, and $h = 6.667$ ft). So we can see that, had the 675-ft curve been banked, the Pennsylvania Railroad's Red Arrow would not have overturned the curve and an accident in 1947 could have been avoided.

So we have shown that we can increase the maximum allowable speed for trains on curves by increasing the superelevation. However there is a limitation to how much a curve can be banked. Limitations on superelevation occur because banking track does not only increases the maximum speed of the trains around a curve, but it also introduces a minimum speed. In fact, banked curves are one example of how a train can derail by going too slowly on certain sections of track [8]. For instance, if the railcar is made too top heavy or the outside wheel is superelevated enough, the force of the weight will begin to tip the railcar over to the inside of the curve at low speeds, even zero mph (see Figure 1.6).

As the weight extends over the inside wheel, the pivot point for the torque changes from the outside wheel to the inside wheel on the curve. In this situation the roles of the two forces and associated torques are in a sense reversed. The weight becomes the destabilizing force trying to underturn the railcar while the centrifugal inertial loading provides a torque toward the outside of the curve counteracting the inward-rolling tendency. Since we have shown that the inertial loading force is proportional to V^2, if the speed of the train is too low, the torque from the weight will overpower the torque from the weak inertial loading force and the train will tip inward. So by using the new force and track geometries in Figure 1.7 to derive new expressions for the torque from the inertial loading force, τ_{inertia}, and the torque due to the railcar weight, τ_{weight}, we can solve for the minimum speed on a superelevated curve.

The expression for the magnitude of the torque from the inertial loading force, $\vec{\tau}_{\text{inertia}} =$

Figure 1.6: A railcar tipping inward on a banked curve due to a high center of gravity and extremely superelevated track.

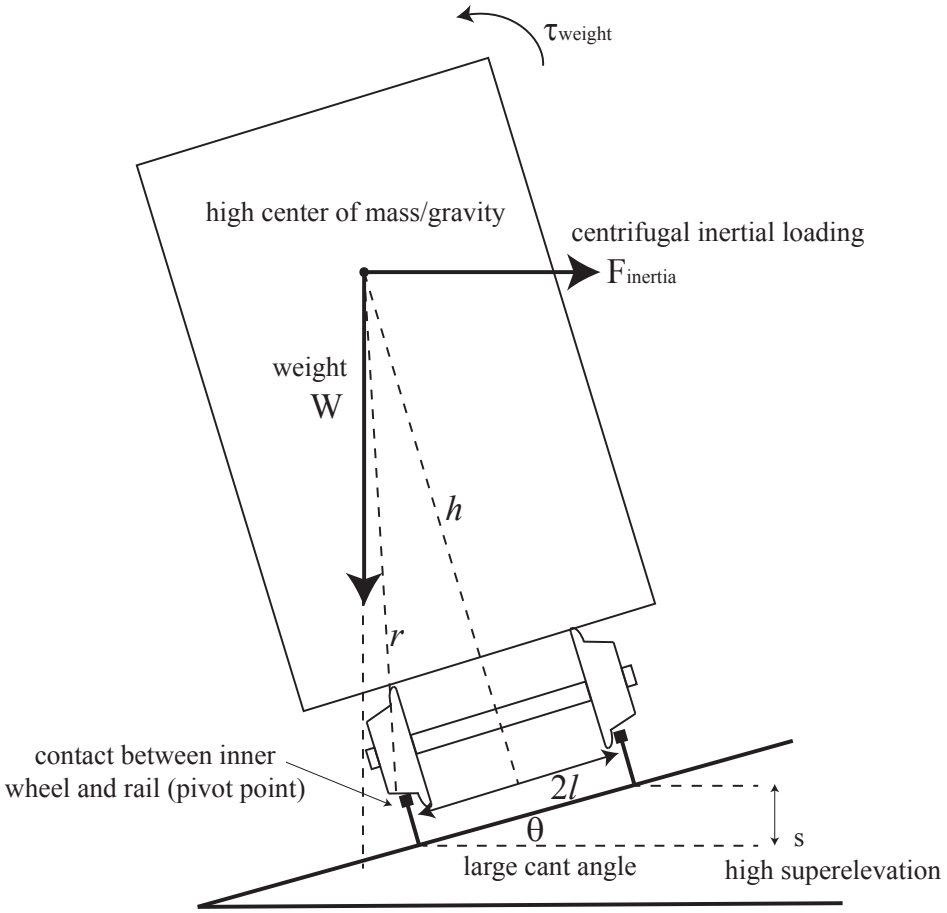

$\vec{F}_{\text{inertia}} \times \vec{r}$, toward the outside of the curve is given by:

$$\begin{aligned}
\vec{\tau}_{\text{inertia}} &= F_{\text{inertia}} r_v \\
&= F_{\text{inertia}} \left[(h - l \tan\theta) \cos\theta + 2l \sin\theta \right] \\
&= F_{\text{inertia}} \left[h \cos\theta - l \sin\theta + 2l \sin\theta \right] \\
&= F_{\text{inertia}} \left[h \cos\theta + l \sin\theta \right] \\
&= \left(\frac{W}{g} \right) \left(V^2 \frac{1}{R} \right) \left[h \cos\theta + l \sin\theta \right]
\end{aligned}$$

And in a similar way we can find the expression for the magnitude of the torque from the weight, $\vec{\tau}_{\text{weight}} = \vec{W} \times \vec{r}$, toward the inside of the circle:

Figure 1.7: Geometry of the forces and torque arm for a top-heavy railcar on a highly banked curve.

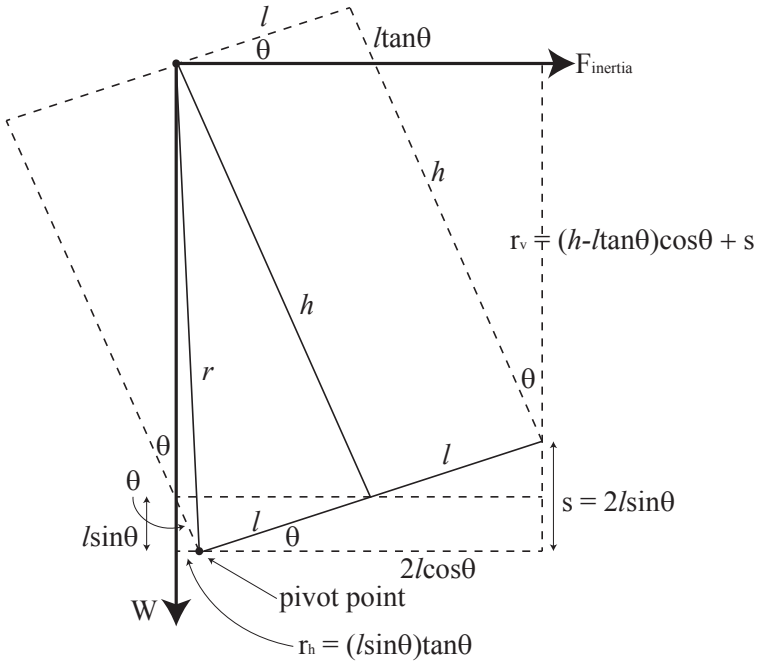

$$\begin{aligned}\vec{\tau}_{\text{weight}} &= W r_h \\ &= W\left[(l\sin\theta)\tan\theta)\right] \\ &= W\left[l\left(\frac{\sin^2\theta}{\cos\theta}\right)\right]\end{aligned}$$

Finally, by setting these two torques, τ_{inertia} and τ_{weight}, equal we can find the critical, or minimum speed that the train must travel in order for the centrifugal inertial loading to counteract the tipping from the weight of the top-heavy train.

$$\begin{aligned}\left(\frac{W}{g}\right)\left(V^2\frac{1}{R}\right)\left[h\cos\theta + l\sin\theta\right] &= W\left[l\left(\frac{\sin^2\theta}{\cos\theta}\right)\right] \\ \left(V^2\frac{1}{gR}\right) &= \frac{l\sin^2\theta}{\cos\theta\left[h\cos\theta + l\sin\theta\right]} \\ V_{min} &= \sqrt{\frac{gRl\sin^2\theta}{\cos\theta\left[h\cos\theta + l\sin\theta\right]}} \qquad (1.5)\end{aligned}$$

When the cant angle, θ equals zero, or in other words when there is no superelevation on the curve, this equation for the minimum speed is also equal to zero. This corroborates the assertion that for flat curves there is no minimum speed; this is only a phenomena that comes as a byproduct of banking curves to allow for faster speeds. So, banked curves introduce the necessity of having minimum speed regulations and these minimum speeds increase as the superelevation height (or cant angle) increase. Therefore, in industrial practice there are limits on the maximum cant allowed on curves to control the unloading of the wheels on the outside or higher rail, especially at low speeds.

1.3 Single Wheelset Derailment on Curves

Before reaching the overturning speed, a slow, heavy freight car is far more likely to derail on a curve by rail rollover, wide gauge, or wheel climb (see Figure 1.8) from a single wheelset. The tendency of a wheel to derail is determined by the forces at the wheel-rail interface, which are often complex and transient in nature. By assuming that these complicated forces at the interface ultimately resolve componentwise into lateral forces, longitudinal forces, and vertical forces, one can reduce the difficulty of predicting thresholds for derailment.

1.3.1 Wheel Climb

Wheel climb occurs when the wheel flange contacts the rail head and the lateral forces toward the outside of the track are greater than the vertical forces pushing the wheelset down onto the rail. Therefore it is natural to characterize and quantify the propensity of a given wheel to derail by wheel climb by defining an L/V ratio, where L is the sum of the lateral forces of the wheel against the rail and V is the sum of the vertical forces on top of the rail at a given time (see Figure 1.9). In general, lateral wheel-rail forces are affected by centrifugal forces on a curve, coupler forces, wheel creep forces, and track geometry, while vertical forces are affected most directly by the loading of the railcar weight and slack and coupler impact forces. The greater the L/V ratio, the more likely the wheel is to climb and a derailment to occur [16].

Although L/V ratios vary with many factors such as the condition of the trucks, rails, and wheels and the dynamic behavior of the car and suspension, there are some rough guidelines that state which L/V ratios might cause derailment [8]. For newly manufactured wheel and rail the L/V ratio can reach approximately 1.29 on straight track before the wheel may climb the rail; however, for curved track instability (or wheel lift) can arise at an L/V ratio of 0.82 or greater. For worn wheel and rail, the maximum safe L/V ratio drops to about 0.75 for

Figure 1.8: Derailment can be caused by (a) rail roll over, (b) wide gauge, or (c) wheel climb.

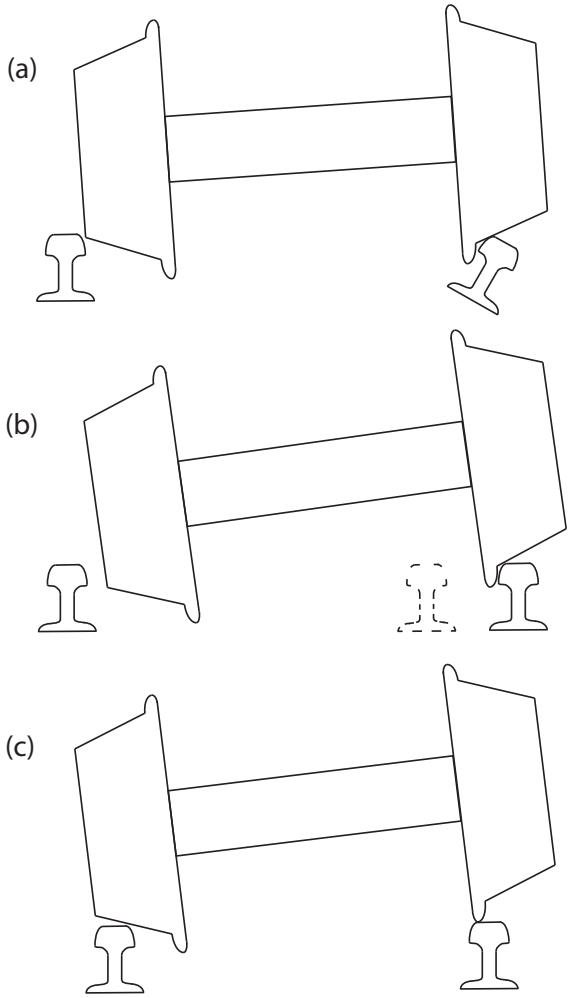

straight track and 0.64 for curved track (at which a poorly constrained or degraded rail may also rollover). So we can see that the wheel-rail profile directly affects the propensity of a wheel to climb a rail. Generally, a new contour wheel will climb a rail before a worn wheel; conversely, worn rail is more prone to wheel climb than new rail.

It is important to note that an instantaneous spike in L/V ratio is less likely to cause derailment than a more prolonged duration or distance of high L/V. In general, a high L/V ratio must persist for at least 6 ft of movement in order for it to potentially cause derailment [16].

In curving, wheel climb can occur either when the train is going too quickly or when the train is going too slowly. In cases where the train is traveling above the maximum curving speed, the excessive centrifugal inertial loading forces the outside wheel flange against the rail on the outside of the curve, producing greater lateral forces. This additional lateral force

Figure 1.9: The lateral (L) and vertical (V) forces at a wheel-rail interface.

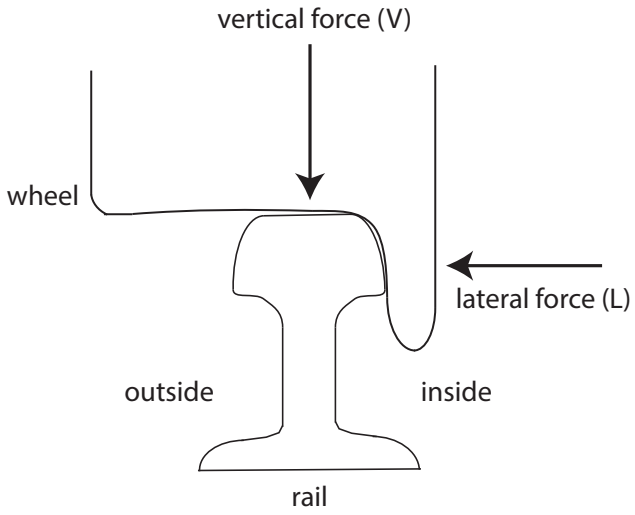

increases the L/V ratio and causes the wheel to climb the rail or the outside rail to overturn. It is in the extreme cases with very high speeds that a car with a higher center of gravity may actually tip over to the outside of the curve (see Section 1.2.2) [16].

In cases where the train is traveling below the minimum curving speed, the train produces insufficient centrifugal inertial loading (in the lateral direction) to keep the outside wheel flange against the outside rail head. So the L/V ratio on the outside wheel falls and the wheel adopts a lateral position toward the inside of the curve. Because of the conicity of the wheel tread, the inside wheel rolls with a greater rolling radius or diameter than the outside wheel. Consequently the inside wheel tend to track ahead of the outside wheel, skewing the handling of the truck towards the outside of the curve. At that point, any number of factors such as rail head discontinuities or bouncing can cause the lead inside wheel to climb the inside rail [16].

1.3.2 Wheel Lift

Wheel lift occurs, regardless of the magnitude of lateral forces, when vertical forces on the rail tend to zero. In extreme cases, the vertical forces could actually point upward away from the rail in which case the wheel is said to be negatively loaded. Wheel lift can occur in situations where severe slack action occurs, severe bouncing occurs, or where harmonic roll is induced in a vehicle [16].

In a curve, if the train is running over the critical speed, the vehicle weight shifts to the outside wheel, reducing the vertical force on the inside wheels and potentially causing wheel

lift on the inside. This is consistent with the scenario in which a fast train overturns on the curve. Conversely, if the vehicle is moving too slowly, the vehicle weight shifts to the inside wheel and wheel lift occurs on the outside.

1.4 Slack and Coupler Impact Forces

Slack is the unrestrained free movement between vehicles in a train. Most rail vehicle couplings have some free slack that allows relative motion between the cars and the truck's draft systems also allows controlled movements between vehicles to help minimize coupler impact force. In a normal train of coupled railcars, each car can move out (plus) or in (minus) 6 inches from their neutral position. This amounts to a total movement of 1 foot per car. For a train of only 100 cars, the entire train can then run out or in 50 ft for a total length change, or slack, of 100 ft [8].

When this slack runs in or out, different cars of the train move at different speeds, creating additional in-train forces that can break a coupling or derail a train. The most significant forces produced by slack action effects are coupler forces that are parallel to the longitudinal axis of the rail vehicle. Slack running in adds additional train compressive forces. These compressive coupler forces, or those forces that tend to push the vehicles in the train together, are called buff forces. On the other hand, slack running out adds additional tension forces. These tensile coupler forces that tend to pull the train vehicles apart are called draft forces [16].

On a curve, too much compressive force (called buff force) can derail a train by buckling or jackknifing cars on the outside of the curve (see Figure 1.10). When a train is compressed on a curve, the couplings are angled, adding additional lateral forces trying to shove cars off the outside rail. This kind of derailment most often occurs on curves at the bottom of hills or grades. Going downhill the train is compressed because braking is concentrated at the front of the train so that the rear cars continue to move forward due to gravity and run in the slack. So jackknife derailments typically occur with heavy dynamic or independent braking, emergency braking from the head end, excessive power in shoving movements, or excessive imbalance of power between lead and helper locomotives [16]. In some cases, the travel limits of the car couplers may result in a car being forced off the track if the curvature is too sharp.

On the other hand, too much tension (called draft force) can cause a train to derail by stringlining on the inside of a curve (see Figure 1.11). Stringline derailments often occurs at slow speeds when the train is stretched by heavy power application in the front that has

Figure 1.10: Train compression buckles or jackknives the train off the outside rail.

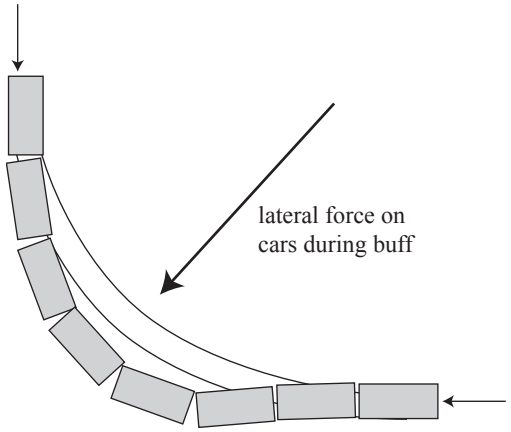

yet to translate through the slack to the end of the train or when brakes are applied to the rear end so that the front of the train continues to move forward and run out the slack [16]. Stringlining forces can also cause inner rail to roll over.

Figure 1.11: Tension force derails the train on the inside rail by stringlining.

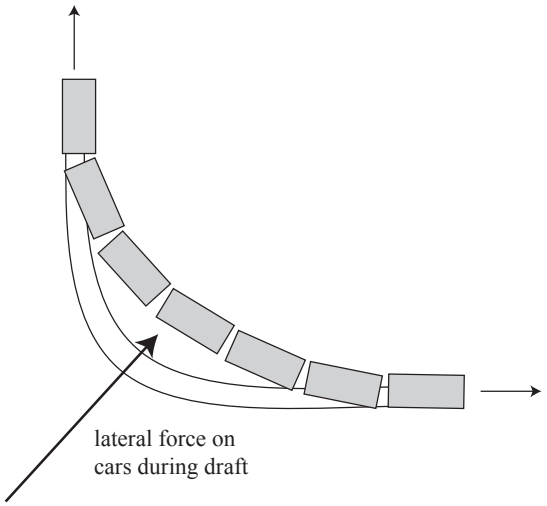

So it is clear that when handling heavy freight trains with many cars, the slack becomes excessive and very difficult to control. So it would be logical to question why trains are designed with so much slack between cars, since it clearly can present a derailment hazard. Train slack serves several purposes, the foremost being that slack allows the train to be flexible and reduces the power required to start a long heavy train. By allowing slack between the cars, the power needed to induce motion must only overcome the static or starting friction of each car at a time; otherwise, one would need enough power to overcome

the starting friction of the entire train at once.

Slack action can be beneficial to train handling, especially when a train is starting from a stopped position. For example, if a locomotive starts pulling a large number of loaded cars from a stopped position, and the cars are in buff, slack allows the locomotive to begin moving the train one car at a time as the slack is stretched out. This reduces the strain on the locomotive traction motors. The same is true if a locomotive starts pushing a large number of loaded cars that are in draft [16]

As freight trains become longer and heavier, buckling, stringlining, and other handling problems become practical limits on the number of railcars in the train and the number of locomotives (driving power) that could be concentrated at the front. One solution is to distribute power by using additional locomotives in the middle or at the end of the train. However, interspersing additional locomotives is not only expensive, but causes delays and losses in loading and unloading cars. Since slack action places a practical limit on the length of trains, it is clear why the rail industry has turned to new ways to carry more freight per train. Instead of adding more cars to the end of already long freight trains, many companies are moving to the use of bi-level cars or double stacked freight containers to increase carrying capacity (see Section 2.4 in the following chapter).

Chapter 2

Parametric Analysis for Speeds on Curved Track

Track that is part of the general railway system in North America is generally designated with a track class, numbered 1 through 9, each with particular regulations concerning track quality and maintenance, signaling, and level of traffic. Sections of rail in track classes 1-5 share both freight and passenger travel and classes 6-9 are dedicated solely to higher speed passenger trains [16]. The higher the track class, the higher the allowable speeds; therefore the structure and quality requirements for higher track classes are more stringent than those for lower track classes. The operating speed limits for track classes 1-5 are specified in 49 C.F.R. 213.9 and those for track classes 6-9 are specified in 40 C.F.R 213.207. The structural specifications for the different track classes are provided in 49 C.F.R 213-Track Safety Standards. Table 2.1 summarizes the industry values for maximum operating speed limits for the nine US track classes.

In the previous chapter, we derived approximate equations for the maximum speed on both a flat and a superelevated horizontal curve of radius R, with rail gauge, $2l$, and height of the center of railcar mass over the rails, h. We found that for flat curves the maximum speed was given by Equation (1.2):

$$V_{\text{max flat}} = \sqrt{\frac{gRl}{h}}$$

And for a superelevated curve of cant angle, θ, the maximum speed was given by Equation (1.4):

$$V_{\text{max elevated}} = \sqrt{\frac{gR[h\sin\theta + l\cos\theta]}{[h\cos\theta - l\sin\theta]}}$$

Table 2.1: Published maximum operating speed limits for US standard gauge track classes.

	Freight Trains (mph)	Passenger Trains (mph)
Class 1 Track	10	15
Class 2 Track	25	30
Class 3 Track	40	60
Class 4 Track	60	80
Class 5 Track	80	90
Class 6 Track	—	110
Class 7 Track	—	125
Class 8 Track	—	160
Class 9 Track	—	200

We proved that the superelevated curve always allows a greater maximum speed than a flat curve; however, we also showed that superelevating the rail introduced the necessity of a minimum speed limit. The expression for this minimum speed on a superelevated curve was given by Equation (1.5):

$$V_{\text{min elevated}} = \sqrt{\frac{gRl\sin^2\theta}{\cos\theta[h\cos\theta + l\sin\theta]}}$$

In this chapter we will explore how these equations can help railway track designers optimize curved sections for particular types of traffic flow. First we will look at how track and railcar geometry affect critical curving speed, focusing on how track optimization can be different when taking into account passenger as opposed to freight travel. We will then discuss how the length and distribution of railcars in the train of vehicles can affect buckling and stringlining slack effects on curves.

2.1 Radius of Curvature

The radius of railroad curves has an important bearing on construction costs and operating costs of railroad track, and in combination with superelevation and other track geometry, determines the maximum safe speed of a curve. Minimum curve radii for railroads are designed to allow a certain operating speed and are constrained by the mechanical ability of the rolling stock to adjust to the curvature. In North America, equipment for unlimited interchange between railroad companies are built to accommodate sharp curves of radius as little as 350-ft, but normally a 410 ft (14 degree) curve is used as a minimum. For handling

of long freight trains, especially those with an uneven distribution of light and heavy cars, a minimum radius of 717-ft (8 degree) is preferred [20].

For passenger trains that must keep commuters to strict timetables, operating speeds are often much higher than those for freight traffic. Therefore curves on dedicated passenger lines are ideally much gentler, with minimum radii of around 6500 ft for intercity express trains operating at the US maximum passenger speed of 125 mph. For dedicated high-speed rail lines, like those in China operating at 218 mph, the minimum curve radius can be as high as 23,000 ft [11]. Table 2.2 summarizes the curving speeds corresponding to minimum freight and passenger curve radii, found from Equations (1.2) and (1.4).

Table 2.2: Critical speeds on flat and superelevated (3°) curves as a function of curve radius, R.

	Curve Radius, R (ft)	$V_{\text{max flat}}$ (mph)	$V_{\text{max elevated}}$ (mph)	$V_{\text{min elevated}}$ (mph)
Freight Boxcar ($h = 7.5$ ft)	350	40	44	3
	410	44	48	3
	717	58	63	4
Passenger Car ($h = 6$ ft)	1200	84	90	6
	6562	196	210	15
	23000	367	395	28

From the maximum curving speed equations derived in the previous chapter, it is clear that a larger radius of curvature allows for a higher maximum allowable speed on both flat and elevated curves increases. From Figure 2.1, we can also see that the maximum speed on a canted curve increases at a faster rate with respect to radius than the maximum speed for a flat curve. This means that a railcar on a curve designed with both a larger radius and a superelevation angle can achieve speeds higher than on a curve with only one of these designs.

From Table 2.2, it is also clear that the radius of curvature has a more significant effect on the maximum speed (for both flat and elevated track) than it does on the minimum speed introduced by a cant angle. Although this result will be discussed further in Section 2.3, it is important to note that these critical speed equations show that increasing the radius of a curve is the best design for increasing speed and traffic flow on track shared by fast passenger and slower freight traffic. This is because both freight and passenger traffic are optimized by increasing radius, while increasing cant angle can introduce minimum speeds too high for slower freight trains to negotiate safely. Although increasing radius is the best track design practice in terms of railcar kinematics, costs of extra real estate and rail can

Figure 2.1: Maximum speed (mph) vs. Radius of curve (ft).

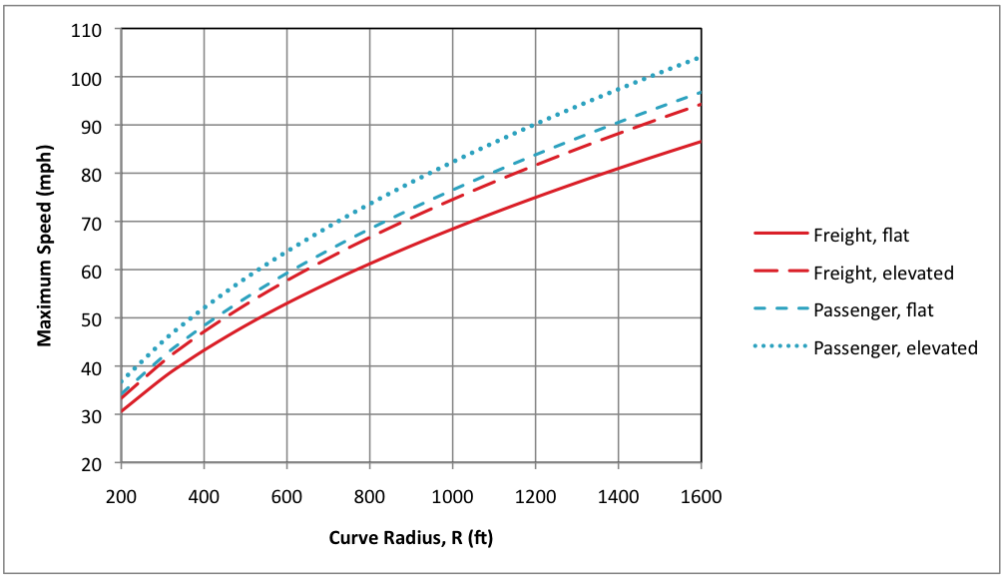

be prohibitive, especially in more crowded urban areas. Therefore, increasing cant angle is often the most economical, if not the only physically practical, option left to engineers and management hoping to increase traffic flow.

2.2 Rail Gauge

Gauge is defined in industry as the perpendicular distance between the insides of adjacent rails measured a distance 5/8 of an inch down from the tops of the rails [16]. Standard gauge of 56.5 inches (4'8-1/2") is used on all track in the general North American railway system and is used almost universally by other railway networks around the world [12]. In industrial practice, rail is maintained so that gauge remains within strict tolerance limits. Published U.S. standard gauge tolerance ranges for passenger and freight track classes are given in Table 2.3 [16] with the corresponding maximum speed ranges derived from Equations (1.2) for flat and (1.4) for superelevated track.

The strict tolerance limits given in Table 2.3 are maintained for a number of reasons. One is that if gauge is not allowed to vary significantly, then the maximum safe speed on the curve is roughly constant (only varying by 1 mph at most). This means that trains can safely approach the curve at the posted speed limit as long as gauge has been maintained to standard. If gauge widens sufficiently, a wheel can drop between the rails and cause a derailment [16]. For a new wheelset and new rail, the gauge would need to widen by at least

Table 2.3: Maximum speed for standard gauge tolerances for passenger and freight classes on flat and superelevated (3°) curves of radius $R = 717$ ft.

		Freight	($h = 7.5$ ft)	Passenger	($h = 6$ ft)
	US Standard Gauge Tolerance Range (in)	$V_{\text{max flat}}$ (mph)	$V_{\text{max elevated}}$ (mph)	$V_{\text{max flat}}$ (mph)	$V_{\text{max elevated}}$ (mph)
Class 1 Track	$56.00 - 58.00$	58-59	63-64	65-66	70-71
Class 2 and 3 Track	$56.00 - 57.75$	58-59	63-64	65-66	70
Class 4 and 5 Track	$56.00 - 57.50$	58-59	63-64	65	70
Class 6, 7, and 8 Track	$56.00 - 57.25$	—	—	65	70
Class 9 Track	$56.25 - 57.25$	—	—	65	70

3.5 inches before a wheel drops between the rails; however, for worn wheel flanges, gauge widening of as little as 2 inches could cause derailment [28]. Derailment by narrowed gauge on curves can also occur, although it is less common. In this case, narrowed gauge can create excessively high lateral wheel-rail forces, causing the wheel to climb the rail and then drop off the track [16].

Despite the risk presented by wide gauge, some railways maintain their standard gauge at the widest tolerance limit on sharp curves to reduce wheel binding. The reason for this is clear when maximum speed is graphed as a function of rail gauge (see Figure 2.2). The critical safe curving speed increases as rail gauge increases for both flat and curved elevated track.

Figure 2.2: Maximum speed (mph) as a function of rail gauge, 2l (in), for flat and superelevated (3°) curves of radius $R = 717$.

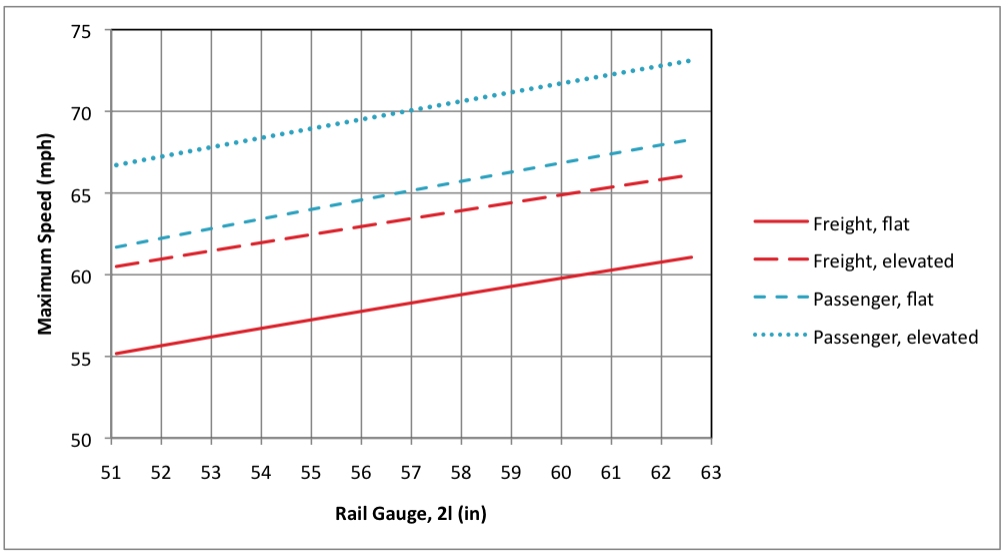

2.2.1 Narrow Gauge

The phrase "narrow gauge railroad" is used to characterize any line of track that is systematically constructed with gauge narrower than the 56.5 inches of standard gauge railways. In some countries narrow gauge is the standard, like the 42-inch gauge in Japan, New Zealand, South Africa, and Tasmania, and the meter (39.4 in) gauge in Malaysia and Thailand [21].

Narrow gauge railroads are usually lighter and smaller in infrastructure construction, use smaller cars and locomotives, and are built with tighter curves. In fact, the sharpest curves tend to be on the narrowest gauge railways, where almost everything is proportionately smaller. Narrow gauge railway can be substantially cheaper in terms of building, equipment, and operating costs, particularly in mountainous terrain where civil engineering work is most costly. Furthermore, the lower costs mean they often serve less populated areas where the demand and traffic potential would not justify the cost of building a standard or broad gauge line.

One problem for narrow gauge railways is that, although they are cheaper in initial construction, the cost of upgrade, whether it is increasing speed or loading, removes most of the price advantage over standard or broad gauge. Narrow gauge railways lack the physical space and robust infrastructure to grow. Their cheap construction means that they are engineered only for their initial traffic demands; while a standard or broad gauge railway could more easily be upgraded to handle heavier, faster traffic. On narrow gauge, speeds and loads hauled cannot increase, so traffic density is significantly limited.

2.2.2 Broad Gauge

The phrase "broad gauge railroad" is used to characterize a track with rail gauge greater than the standard gauge of 56.5 inches. Russian gauge or CIS gauge (59.8 in) is the second most widely used gauge in the world, behind U.S. standard gauge. CIS gauge spans the whole of the former Soviet Union bloc, including the Baltic states and Mongolia. Railroads in India adopted an even wider gauge of 66.0 inches since it was thought necessary to keep trains stable in the face of strong monsoon winds. This broad gauge is still commonly used in India, Pakistan, Bangladesh, Sri Lanka, Argentina and Chile [11].

Broad gauge tracks usually support greater axle loads compared to standard gauge tracks because broad gauge construction uses heavier rails [21]. Broad gauge offers an advantage to freight movement. In India, trains on the broadest gauge can carry standard shipping containers double-stacked on standard flatcars, which is more economical than single containers. In contrast, standard-gauge railways in North America and elsewhere must use special double-stack cars to lower the center of gravity and reduce the loading requirements. Broad

gauge also increases the maximum critical curving speed compared to standard gauge tracks, so that heavier freight trains can run faster and therefore more efficiently. The derived maximum critical curving speed for sample narrow and broad gauge systems are summarized in Table 2.4.

Table 2.4: Maximum speed for freight cars ($h = 7.5$ ft) on narrow, standard, and broad world gauge systems ($R = 717$ ft).

	Gauge (in)	$V_{\text{max flat}}$ (mph)	$V_{\text{max elevated}}$ (mph)
Malaysia and Thailand Narrow Gauge	39.4	48	57
Japan Narrow Gauge	42.0	50	63
US Standard Gauge	56.5	58	63
Russia (CIS) Broad Gauge	59.8	60	65
India Broad Gauge	66.0	63	68

Broad and narrow gauge railways cannot interchange rolling stock freely with the standard gauge lines with which they link. Therefore, where there are breaks in gauge, or changes from one gauge system to another, transfers of passengers and freight require time consuming manual labour or substantial capital expenditure. Not having a uniform gauge throughout a network makes it difficult to move rolling stock to where it is needed in times of peak demand. Smaller railroad companies operating on a standard gauge can rent rolling stock from larger companies during times of overflow, without increasing their year-round overhead. On the other hand, broad or narrow gauge railroads must own enough rolling stock to meet their own peak demand. This surplus equipment generates no cash flow during periods of low demand. Therefore, it is advantageous to adopt one standard gauge throughout a rail transport system so that interoperability of rolling stock is possible. Most new railroad lines installed around the world now conform to U.S. standard gauge measurements. This widespread use of standard gauge fosters competition among manufacturers of trains and track who also benefit from economy of scale. This lowers prices and therefore reduces the cost of new track construction.

2.3 Superelevation Angle

Chapter 1 discussed how maximum speed on a curve is the speed at which the outward torque due to the centrifugal inertial loading counteracts the inward torque due to the weight. Put another way, the equilibrium speed occurs when the resultant of the weight and the centrifugal force is perpendicular to the plane of the track so that the components

of both forces in the plane of the track are balanced [6]. We have shown that increasing the cant angle for the curve increases the maximum speed allowed on the curve, but we have also shown that this cant angle introduces a minimum speed limit as well. If it were possible to operate all classes of traffic at the same speed on a curve, the ideal condition for smooth riding and minimum rail wear would be obtained by elevating the outside rail of the curve until equilibrium is reached. However, curved track must handle several classes of traffic operating at various speeds. Therefore slower trains running closer to the minimum critical curving speed load and wear the inside rail, whereas high-speed trains running close to the maximum speed wear the outside rail. Figure 2.3 shows the maximum curving speed as a function of cant angle while Figure 2.4 shows the minimum curving speed as a function of cant angle.

Figure 2.3: Maximum speed (mph) as a function of superelevation angle (°) for curves of radius $R = 717$.

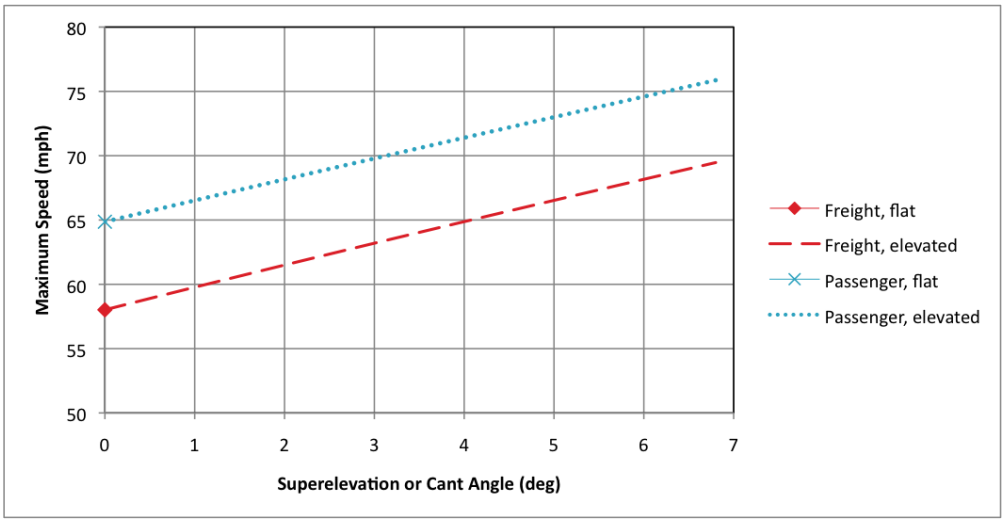

These graphs illustrate the optimization problem that face many track designers, particularly in the U.S. To increase traffic flow and efficiency on existing track, often the cheapest and most efficient solution to higher speeds is to increase the elevation of the outside of the track. However, this increased elevation presents a problem for slow freight traffic, that also in the interest of increased efficiency, are made longer and heavier. So in summary, canting of curved track allows for greater maximum speeds and is particularly desirable for short, light passenger trains that must keep to tight commuting schedules. However, these same cant angles present a problem for slower, longer, and more top-heavy freight trains because cant introduces a minimum speed limit and excessive loading of the wheel on the outside rail. This presents a particular challenge in designing rail corridors where freight and passenger

Figure 2.4: Minimum speed (mph) as a function of superelevation angle (°) for curves of radius $R = 717$.

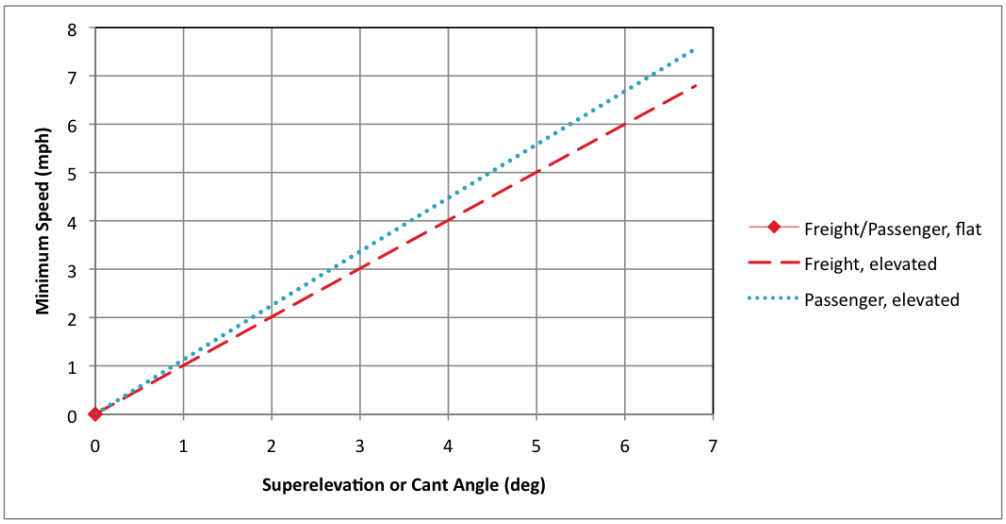

trains share track (which is a common practice in the United States).

This balance between increasing maximum curving speed and introducing minimum speed limits becomes especially important when considering rail corridors in much of the United States. This is because Amtrak, the U.S. passenger rail service, often rents running rights on rail owned and maintained by freight companies for freight traffic. This means that lighter and faster passenger trains, which would like much higher maximum curving speed limits and can afford to maintain a high minimum speed, must run on track optimized for slower, longer, and heavier freight traffic, which run the risk of tipping inward on highly banked curves. To solve this optimization conflict, Amtrak's 150-mph (214-km/h) Acela Express is installed with a self-tilting truck and suspension system that creates its own bank angle [19]. The Acela is able to tilt an extra 4.2 degrees so that when operating on curved track with a superelevation of 2 inches, the Acela can speed as if it is on a track that is raised an additional 7 in, for a total superelevation height of 9 inches [8]. From Equation (1.4), we find that the tilting action of the Acela train (with estimated center of mass height, $h = 3$ ft above the rail) allows it to traverse a curve of radius $R = 717$ ft with speed limit of 95 mph (corresponding to a superelevation height of 2 in) at a speed of up to 108 mph (corresponding to a superelevation height of 8 in).

Tilting trains can help solve the problem of shared rail between freight and passenger services, but it is far from ideal. One reason is that sudden changes from one superelevation to another can result in undesirable roll dynamics in a vehicle [16]. Therefore, in more open areas where real estate is not too expensive, the first choice of most rail companies is to

redesign curves with larger radii, since we have seen that increasing the radius increases maximum curving speed while having little effect on the minimum operating speed.

2.4 Railcar Dimensions (Height)

So far we have analyzed three parameters related to track geometry - namely curving radius, track gauge, and cant angle - that directly affect the critical curving speed. However, improving track design is not the only option for railroad managers and engineers who want to increase speeds and the flow of traffic on curved sections of track. Railcar dimensions, particularly the height of the center of mass of the railcar above the tops of the rails, also affect the curving speed.

In Chapter 1, we showed that the car body assumes a radial position on a curve. When the railcar is traveling at a speed over the maximum curving speed, the superelevation and other designs of the rail may not be completely effective in balancing out the centrifugal inertial loading created by the circular motion of the car. With this unbalanced force acting at the center of gravity of the car body, the body will be displaced outwardly and can tilt toward the outside of the curve [6]. From the maximum speed equations for flat and superelevated curves, it is clear that decreasing the height of the center of mass of the car body above the rail increases the maximum curving speed (see Figure 2.5). Because of this relationship, one might imagine that railcar designers who want to optimize the flow of traffic would design low, squat cars that can negotiate curves safely at a high speed. However, Figure 2.5 also shows that the maximum curving speed function has the steepest curve and is therefore most sensitive to changes in center of mass height at smaller values of h, or closer to the top of the rail. This means that speed limits for short, squat cars would vary dramatically given their loading because increasing or decreasing the center of mass by less than a foot could result in at least a 5 mph difference in the critical speed. Although it is true that high-speed, intercity passenger trains are designed to keep an aerodynamic and low profile, the general trend in the freight and commuter railway industries is actually to increase the center of mass height of the cars to avoid uncertainty in the speed limit.

A standard intermodal freight or ISO container in the United States is designed so that it can be moved from one mode of transport, such as rail, truck, or ship, to another without unloading and reloading contents. Lengths of these containers vary from 8 to 56 feet and heights from 8 feet to 9 feet 6 inches [4]. So taking a standard boxcar to have a height of 8 or 8 1/2 feet, and accounting for the wheelset and truck on which the containers sit which add additional height, the external height of a standard boxcar above the rails is approximately

Figure 2.5: Maximum speed (mph) as a function of the railcar center of mass height (ft) for flat and superelevated (3°) curves of radius $R = 717$ ft.

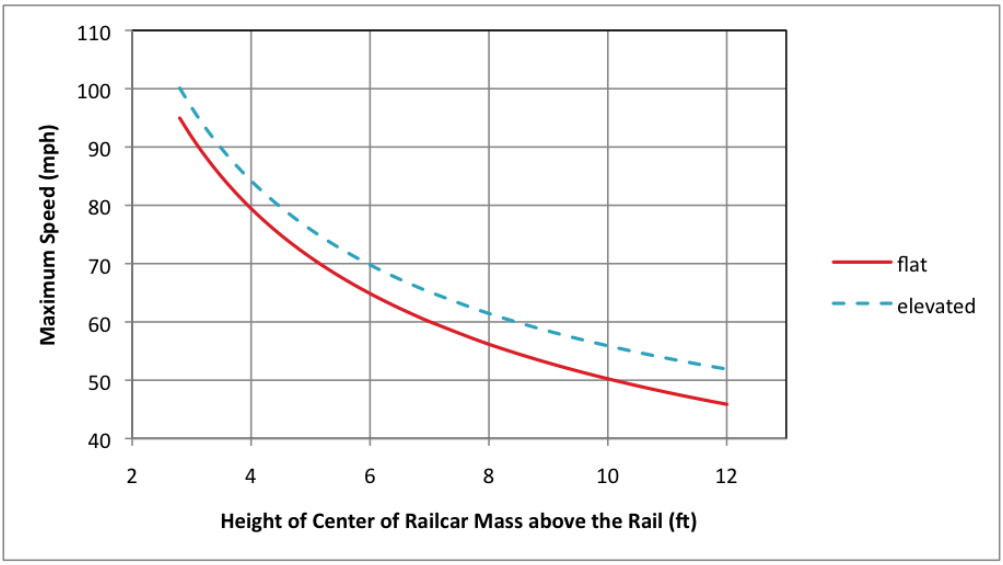

15 feet [22]. Therefore, it is clear that, for a uniformly-filled car, the center of mass will be about 7 or 7 1/2 feet above the rail, where the maximum speed for curving as a function of center of mass height is just leveling off. In fact, this means that adding additional height beyond the single container has little impact on the critical speed. Therefore, many railroad companies can sacrifice only a few mph of speed for increased cargo. This has led to a dramatic rise in the use of bi-level cars for some high-volume, slower speed passenger services and double-stacked containers for freight.

2.4.1 Bi-level Passenger Cars

The bilevel car is a type of rail car that has two levels of passenger accommodation, as opposed to one, increasing passenger capacity (in example cases of up to 57% per car) [24]. To keep down costs and maintain safety, the double-deck design usually includes lowering the bottom floor to below the top level of the wheels, closer to the rails, and then adding an upper floor above. Such a design minimizes car height. For example, a typical Amtrak single-level passenger or Amfleet car, is 12 feet 8 inches tall relative to the top of the rail, 10 feet 6 inches wide, and 85 feet 4 inches in length. A Bombardier Amtrak Superliner bi-level car can carry significantly more passengers but is less than 4 feet taller than the single-level car, at 16 feet 2 inches above the top of the rail [10]. This lower design allows these cars to run on existing track without significant infrastructure changes because they can fit under the

already established bridges, tunnels, and power lines. This lower centre of gravity also lets bi-level trains continue at about the same speed on curves as their single-level counterparts.

It should be mentioned that the height of the cars can limit their use on lines that use more flimsy narrow gauge that cannot handle the increased load of two-level cars. Furthermore, high passenger capacity can create flow and problems at train stations when much larger numbers of passengers try to board or disembark at the same time and can cause problems in an evacuation situation. However, the use of double-decker carriages, where feasible, can resolve capacity problems on a railway, avoiding other options which have an associated infrastructure cost such as longer trains (which require longer station platforms and can introduce slack effects), more trains per hour (which the signaling or safety requirements may not allow) or adding extra tracks besides the existing line. This means that bilevel trains often have a lower operating cost per passenger and, in addition, may be more energy efficient [24].

2.4.2 Double-Stacked Freight Cars

Increasing the carrying capacity of long-haul freight trains is a different optimization problem than increasing the speed and number of trains on passenger tracks. By using double-stacked containers railroad companies can increase freight efficiency by carrying more cargo per trip without adding cars on the end of already lengthy trains, adding uncontrollable slack forces. One of the advantages to using double-stacking to increasing volume of freight along a section of track is that it requires few modifications to the rail. As long as the curves are not banked at too great of an angle (which could cause the now heavier train's weight to tip the railcar over the inside rail), the only other concern for double-stacked cars is the higher center of mass. But we have seen that the critical speed varies little once the center of mass is higher than about 8 feet above the track (only slightly higher than the center of mass of a single container).

The major expense of double stacking is that higher cars requires a higher clearance above the tracks than do other forms of rail freight. So like bi-level passenger cars, which have a floor below the wheels, double-stacking standard ISO intermodal containers requires special suspensions and bogies. Even with these modified trucks, the height of double-stacked freight vehicles are higher on average than bi-level passenger cars. In the extreme, double-stack loads are permitted to reach 20 feet 3 inches above the top of the rail [2]. Another interesting feature of the cars specially constructed for double-stack intermodal freight is that many are articulated; or in other words share wheels between the car's units. This can reduces slack action on long trains and improves the ride quality for fragile cargo.

Double-stack freight cars are most common in North America where over-rail electrification is less widespread and there are therefore more manageable overhead clearances. In addition, the U.S. railroad network sees some of the heaviest intermodal traffic in the world. Heavy traffic means a more likely pay-off on large investment to raise bridges and tunnel clearances as well as to remove other obstacles to allow greater use of double stack trains on direct routes.

2.5 Train Length and Railcar Distribution

Parameters that do not appear in the kinematic analysis (derived in the previous chapter from the forces on a single railcar) are the length and distribution of the vehicles in the train. The number of railcars and their type have tremendous consequence for certain curving situations, and although these relationships have not been mathematically derived in the previous chapter, I would be remiss if I did not address them at least qualitatively as they must be considered when designing curved sections of track.

Section 1.4 in the previous chapter discussed how spacing between railcars can lead to coupler impact forces that can buckle or stringline a train in compression or tension respectively. The occurrence and magnitude of these coupler forces depends on a number of factors including, but not limited to, changes in grade (incline) and curvature, the difference between braking or tractive effort by the locomotive at the front and the cars at the back of the train, differences in braking performance between empty and loaded cars, the speed of the train, and the length, weight, and arrangement of cars in the train [16]. This is especially important for freight trains, which unlike passenger trains made up of chains of uniform cars, are made up of many types of cars of different designs (including length and height) and different loads.

Speed and length of the train affect the coupler impact forces caused by slack action. Slower trains tend to produce higher coupler impact forces than faster trains during braking [15]. This is because slower trains produce higher braking forces, since brake shoe friction is higher at lower speeds. However, every vehicle in a train does not travel at the same speed because of the running in and out of slack. Therefore, as brakes are applied from the locomotive at the front of the train, the front end slows first and at this slower speed gains greater braking force. This creates a speed (and braking) differential between the cars in the front and the cars in the rear. The cars in the rear, which are moving at a faster speed, will collide or push against the coupling of the many cars in front of them. Because the rear cars run into the main body of the train, which is more massive in comparison, they experience

more severe coupler impact forces [15]. So it is clear that the longer the train, the greater the speed differential between front and back ends, the greater the mass of cars before the cars in the back, and therefore the greater the coupler forces at the back.

Another important factor is the distribution of loaded and unloaded cars in the train of vehicles. Not only are freight trains made up of heterogeneous car designs, the distribution of cars in the freight train changes along long-haul routes as deliveries are made and cars are decoupled and coupled to the train. This means that the slack dynamics of a train may change after each stop, which can create unpredictable and difficult handling problems for the engineer. Coupling and decoupling freight cars is a time-consuming and costly process, so in order to decrease transfer expenses and maintain delivery schedules rail companies often load the train with the first deliveries in the back and the cars going to the final destination at the front of the train. However, this is not always the ideal distribution of cars. In fact, this often means putting the loaded delivery cars at the back of the train for easy access and empty cars being re-distributed along the system towards the front of the train. This can cause severe slack problems on curves and inclines as a train with empty cars in the front and loads in the rear tends to produce higher coupler impact forces than a train which loads in the front and empties in the rear [15].

Empty cars weigh less and therefore produce higher braking ratios. Because they have a smaller inertial resistance, empty cars have a higher deceleration rate. Therefore, if the empty cars are in the front of the train, followed by laden cars, braking causes the empty cars in front to reduce speed even more quickly than the loaded cars in the rear. In this way a head-end brake application from the locomotive results in a relatively large speed differential between the cars as the slack runs-in, resulting in higher coupler impact forces, in some cases sufficient to cause a derailment [16]. If the train is in a curve, derailment is even more likely because of the eccentricity of the coupler impact forces. Then the heavy back end of the train compressed the front, there is decreased flexibility in the couplers so they can less easily turn.

This would suggest that in best industrial practice, railroads should load any empty cars at the very rear of the train. However, this is costly and time-consuming because loaded cars at delivery would have to be decoupled from the middle of the train and then the train put back together before continuing to the next stop. Because of this, many freight companies take short-cuts that can nominally increase risk of derailment.

Not just the difference in weight between the front and ends of the train, but even the interspersion of one empty car can cause problems with slack action. This is because empty cars weight less and therefore have a lower vertical load, V, and a higher L/V ratio [8]. As a result, empty cars have a greater tendency to derail by wheel climb (see Section 1.3.1).

One long, lightly loaded or empty car between two short heavy cars in a curve can jackknife (derail to the outside) if buff coupler forces are severe enough to force the car over the outside rail. Whereas, a short empty car between long, loaded cars can cause the empty car to stringline (derail to the inside) if draft coupler forces are severe enough to pull the car over the inside rail (see Figure 2.6).

Figure 2.6: On a curve, (a) a long car between short cars can cause jackknifing, while (b) a short car between long cars can cause stringlining.

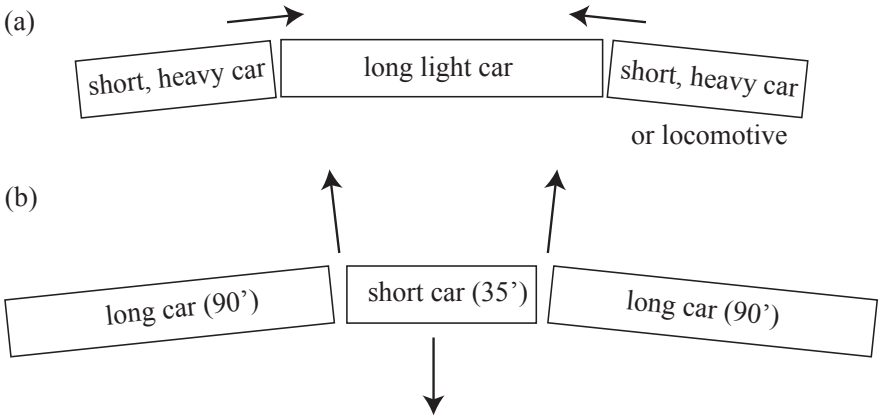

In addition to an uneven distribution of cars in the train, unbalanced or improperly secured cargo (or lading) can affect the slack action of the train of vehicles on a curve. We have already seen that loads with a higher center of gravity must curve at lower speeds or risk a higher likelihood of wheel climb or lift. In addition, improperly secured lading can shift during transit and cause undesirable vehicle dynamics which result in derailment. Derailment usually occurs when the shifted or eccentric load is combined with dynamic train forces such as centrifugal inertial loading or variations in track superelevation [16]. The lighter end of the train or lighter side of the car is more likely to derail for the same reasons that an empty car is more likely to derail - because of lower vertical wheel forces and a higher L/V ratio. Sloshing liquids in partially filled tank cars are a good example of this phenomena.

2.6 Best Practices for Curved Track Design

It is clear that the optimal curved track design depends on the character of the traffic along the route. Optimizing corridors shared by both freight and passenger rail is difficult because slower, heavier, and longer freight trains exhibit different dynamics than faster, lighter, and

shorter passenger trains. However, basic kinematics can inform certain general practices for railroad managers and engineers optimizing curved track.

First, track geometry - including radius of curvature, superelevation height or cant angle, and gauge - affects the safe speed at which a railcar can traverse a curve. In order to increase maximum curving speed for faster, lighter commuter trains without compromising the stability of longer, heavier, and slower freight traffic, the best practice is to redesign track with gentler curves of larger radius. However, construction of brand new track can be disruptive to traffic flow and extremely expensive due to infrastructure and real estate costs. Therefore, banking of the outside rail on the curve by a small degree can increase maximum curving speeds for passenger trains, while introducing a fairly low minimum speed limit for freight. For even faster express passenger trains, tilting suspension systems can be introduces to self-bank on shared corridors. In general, rail gauge is standardized across the national network to allow for interchange of rolling stock between companies, reducing travel time between regions and requiring less overhead and capital. Therefore, rail gauge is not a variable in track design but is an important focus of maintenance.

In addition to track geometries, railcar height also affects critical curving speed. Although increasing height decreases the maximum speed, beyond a certain height the effect becomes negligible. Therefore, although the highest speeds demanded by intercity passenger rail require low-profile railcars, most capacity and traffic flow problems on curved track are best solved by constructing two-level cars for both commuter and long-haul freight rail.

Lastly, the length of the train and the distribution of different cars within the train affect stability on curves. Slack forces are not a significant factor for shorter, lighter, and homogeneous passenger trains. However, they can present a significant problem for longer, heavier freight trains that often carry many types of cars each with a different load. In general, these forces are not controlled by track design but instead by close attention by railroad management to train composition in the coupling yard. The kinematic and parametric analysis presented in these first two chapters cautions that time-saving shortcuts such as coupling the cars by location rather than by optimal distribution (with empties in back and loads toward the front) can result in derailments. These derailments, which damage the cargo being transported, the rail, and the rolling stock itself, can in the long-run be more costly than maintaining good practice.

Chapter 3

Kinematic Analysis of the Wheelset on Straight Track

In Chapter 1, we saw how the basic wheelset geometry of a fixed axle, coned tread, and flange affects the motion of the railcar on both flat and superelevated horizontal curves. From this analysis, it is clear that on gentle curves the conicity provides the main form of guidance. In curving, the axle can adopt a radial position and the coning allows the wheel on the outside of the curve to travel the longer distance at the same angular speed as the inner wheel. This chapter will discuss how the coning of the wheel treads does not just allow trains to traverse curves; it also contributes to the motion of the railway vehicle on straight, or tangent track. However, absent from this discussion will be the affect of flange contact. In the previous chapter it was clear that when approaching curves at too high of a speed, the coned wheelset adopts the radial position with maximum lateral displacement, causing the flange to contact the rail and act as a pivot point for the railcars centrifugal inertial loading. On straight track, common belief might suggest that the wheels are kept on the track by the flanges; but in actuality the flanges make little contact with the track in ideal straight running and when they do, most of the contact is sliding. The rubbing of a flange on the track dissipates large amounts of energy, mainly as heat and noise, and if sustained would lead to excessive wheel wear. In practice, track and wheelset are designed to minimize this contact, so a close examination of the motion of a railway vehicle on straight track in ideal running is focused on the affect of a tapered tread and largely ignores the geometry of the flange [7].

As long as the wheelset is moving on a perfectly straight track with axle center coinciding with the middle of the track, the movement of any un-coned or cylindrical wheel will be similar to the movement of a coned wheel; both will roll forward indefinitely. However, if the

wheelset gets disturbed to one side due to any problems with track, vehicle, or engineman-ship, the un-coned wheel would provide no steering to correct for this disturbance and the wheel would simply run off the rail in the direction of the disturbance. On the other hand, when a coned wheel moves forward on straight track, any slight lateral displacement by an amount y known as the tracking error will push one wheel onto a larger running radius (like the wheel is effectively adopting a slight radial position) by a factor dictated by the conicity of the wheel tread. The angular velocity is the same for both wheels since they are coupled via a rigid axle, so this wheel rolling on the larger radius will cover a greater distance than the wheel rolling on the smaller radius. This yaws the axle and introducing a tendency to roll back toward the center of the track. The wheelset overshoots the center of the track and is then displaced laterally the other way [26]. This result is a kinematic oscillation in both lateral position and axle yaw as the train moves forward along the track (see Figure 3.1).

Figure 3.1: Oscillation of a coned wheelset down straight track.

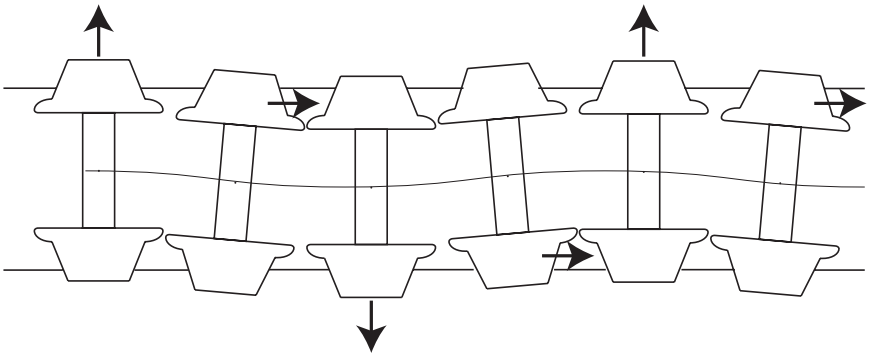

This periodic motion in lateral displacement and yaw of the wheelset on straight track is known as "hunting oscillation." This motion arises from the interaction between the adhesion or frictional forces that accelerate the wheelset in the direction of its displacement and other contact forces between the wheelset and rail that oppose this motion and restore the wheelset to the center of the track [26]. These opposing contact forces require advanced contact mechanical theory to characterize fully but we can estimate their total lateral, vertical, and longitudinal components which we will call "inertial forces." At low forward speeds, the inertial forces between the coned wheelset and rail are greater in magnitude than the adhesion forces so that oscillations in lateral displacement and yaw are damped out. However, as the running speed of the wheelset increases the adhesion forces and inertial forces become comparable in magnitude. At a critical speed where the adhesion forces and the inertial forces are equal, the oscillations persist and the wheelset is said to be hunting. Above this speed, the adhesion forces overcome the inertial forces that would return the wheelset to

the center of the track. At these speeds the oscillations in lateral displacement and yaw are amplified by the frictional forces so that the periodic motion of the wheelset can be violent, damaging track and wheels and potentially causing derailment.

So the same coned geometry that provides stability for curving also helps the wheelset stay on straight track should it be disturbed in any way. These oscillations explain the distinctive side to side motion of trains as they rumble down a track. For low speeds they are a source of stability and an endearing feature of rail travel; however for high speeds they can be a dangerous source of instability. This means that the onset of amplified hunting oscillation limits the operating speeds of steel-wheeled trains. This chapter explore the kinematics of railroad wheelsets on straight track by first describing the periodic lateral displacement and axle yaw motions and then by estimating the critical speed at which hunting oscillations are amplified and the straight running motion of the railcar becomes unstable.

3.1 Kinematic Oscillation in Displacement and Yaw

A kinematic description of the lateral and angular sinusoidal motions is based on the geometry of a wheelset running on straight track and therefore makes a number of simplifying assumptions by neglecting the forces causing the motion. In the following considerations, a single rigid wheelset (not attached to a train or truck) is modeled. The wheelset moves forward at a constant speed, V, in the x direction down a straight and level track. The wheelset never slows down since we assume there are no forces acting on it along the longitudinal or x-axis. We also assume that the downward vertical forces on the wheelset are sufficient to ensure that the wheels adhere to and roll along the track without slipping.

3.1.1 Lateral Displacement

We define the path of the wheel set relative to the straight track by a function $y(x)$ where x is the progress along the track. If initially the wheelset is centered on the railroad track then the effective diameters of each wheel are the same and the wheelset rolls down the track in a perfectly straight line forever. If the wheelset is a little off-center so that the effective diameters or radii of the treads are different, then the wheelset is perturbed from its straight path by a lateral distance, y, and starts to return to the center of the track in a curve of radius R that is given by rearranging Redtenbacher's formula (Equation 1.1) for a wheelset on a gentle curve:

$$\frac{1}{R} = \frac{\alpha}{rl} y$$

where again α is the wheelset conicity, $2l$ is the rail gauge, and r is the average running radius of the centered wheelset.

We can use this equation for a curve to introduce a second order differential equation describing the oscillating motion of the wheelset given a slight lateral (or radially-positioned) displacement. It is a geometric fact that the second derivative of the equation of a circle with radius R centered at a defined origin is equal to $\frac{1}{R}$. Therefore, provided that the direction of motion remains more or less parallel to the rails, the curvature of the path may be related to the second derivative of y with respect to x as approximately:

$$\left|\frac{\mathrm{d}^2 y}{\mathrm{d}\, x^2}\right| \approx \frac{1}{R}$$

Then it follows that the trajectory along the track (see Figure 3.2) is governed by the familiar differential equation:[1]

$$\frac{\mathrm{d}^2 y}{\mathrm{d}\, x^2} = -\frac{\alpha}{rl} y$$
$$\frac{\mathrm{d}^2 y}{\mathrm{d}\, x^2} + \frac{\alpha}{rl} y = 0$$

If the wheelset is initially perturbed in purely the lateral direction by the maximum lateral displacement allowed by the geometry of the wheelset and rails, $y_{o_{max}}$, then $y(0) = y_{o_{max}}$ and the solution to this differential equation is simple harmonic motion (see Figure 3.2):

$$y = y_o \cos\left(\frac{2\pi}{\lambda} x\right) \tag{3.1}$$

where y_o is the amplitude of the lateral displacement and λ is the wavelength of the harmonic oscillation given by Klingel's formula, derived in 1883 [13]:

$$\lambda = 2\pi\sqrt{\frac{rl}{\alpha}} \tag{3.2}$$

The amplitude of the wheelset oscillation, y_o, is constrained by half of the standard play between the wheelset and the track. The standard play, σ_s, of the wheelset can be found by subtracting the axle width (or wheel gauge), w, and the flange thickness of both wheels, $2t$,

[1]It should be noted that $\frac{\mathrm{d}^2 y}{\mathrm{d}\, x^2}$ is negative when y is positive and that the equation $\frac{1}{R} = \frac{\alpha}{rl} y$ is not true when y is negative (since the radius, R is defined mathematically as a positive quantity). However after the R is eliminated in combining the two equations, the resulting equation holds for both positive and negative y.

Figure 3.2: Sinusoidal motion of the center of gravity of a coned wheelset.

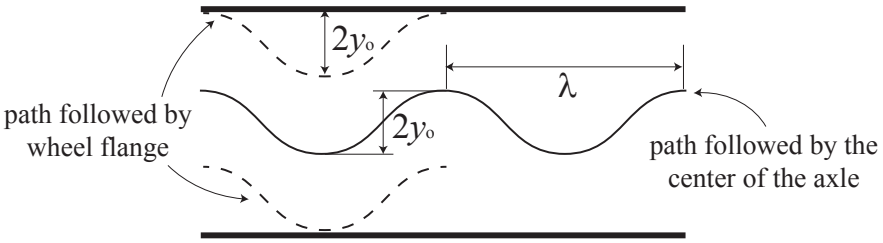

from the track gauge, $2l$ (see Figure 3.3). This yields the equation:

$$\sigma_s = 2l - (w + 2t)$$

So the amplitude of the wheelset oscillation is constrained by half of this standard play:

$$y_{o_{max}} = \frac{1}{2}\sigma_s = l - \frac{w}{2} - t \tag{3.3}$$

Figure 3.3: Play between the wheelset and track.

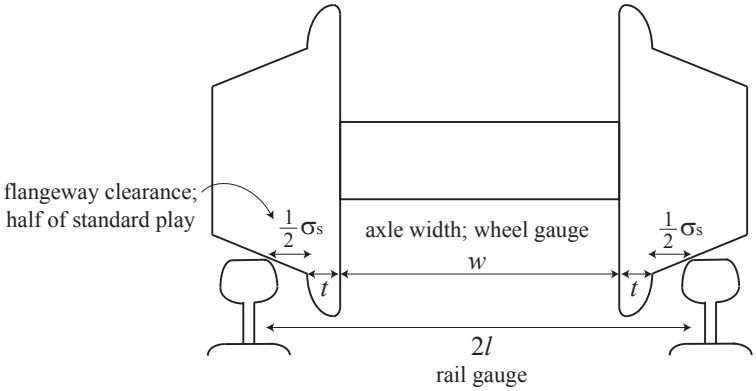

We can look at the change in the periodicity of the oscillation in another way by introducing the wheelset speed, V, to Equation (3.2) for the oscillation wavelength. In this way, we can find the time domain frequency of the Klingel oscillation:

$$f = \frac{V}{\lambda} = \frac{V}{2\pi}\sqrt{\frac{\alpha}{rl}} \tag{3.4}$$

This frequency of oscillation, which depends most heavily on the speed of the railcar, contributes to the whole-body vibration exposure of passengers and can in extreme cases cause discomfort or injury [18]. The following chapter explores the connection between oscillation

frequency and the riding comfort of passengers in more detail, but here we will note that at most safe operating speeds, the frequency of oscillation is at worst noticeable yet tolerable.

3.1.2 Axle Yaw

If the forward motion of the axle down the track is substantially parallel with the rails, the angular displacement of the wheelset about the center of the rails, or axle yaw, θ is given by

$$\theta = \frac{\mathrm{d}\, y}{\mathrm{d}\, x}$$

Differentiating both sides with respect to the progress along the track, x, yields the expression

$$\frac{\mathrm{d}\, \theta}{\mathrm{d}\, x} = \frac{\mathrm{d}^2\, y}{\mathrm{d}\, x^2} = -\left(\frac{\alpha}{rl}\right) y \tag{3.5}$$

By again taking the derivative and substituting in for θ, it is clear that the angular deflection also follows simple harmonic motion.

$$\frac{\mathrm{d}^2\, \theta}{\mathrm{d}\, x^2} = -\left(\frac{\alpha}{rl}\right) \frac{\mathrm{d}\, y}{\mathrm{d}\, x} = -\left(\frac{\alpha}{rl}\right) \theta$$

Given that the wheelset is initially perturbed only in the lateral direction so that the wheelset is not yawed at its initial position, we have the initial condition $\theta(0) = 0$ and the solution to the differential equation is:

$$\theta = \theta_o \sin\left(\frac{2\pi}{\lambda} x\right) \tag{3.6}$$

where θ_o is the amplitude of the axle yaw oscillation and λ is the wavelength of the axle yaw oscillation. The wavelength of the axle yaw oscillation is the same as the wavelength of the lateral displacement because both are dependent only on the geometry of the wheelset and rail. So λ is given by Equation (3.2).

$$\lambda = 2\pi\sqrt{\frac{rl}{\alpha}}$$

Just as the amplitude of the harmonic oscillation of the lateral displacement is constrained by the standard play between the wheelset flanges and the rail, so is the maximum amplitude of the axle yaw oscillation. From the rail and wheelset geometries (see Figure 3.4), the

maximum yaw is given by:

$$\theta_{o_{max}} = \sin^{-1}\left(\frac{\sigma_s}{r_{outer}}\right) = \sin^{-1}\left(\frac{2y_{o_{max}}}{r + \alpha y_{o_{max}}}\right) \tag{3.7}$$

Figure 3.4: A wheelset at maximum yaw between the rails.

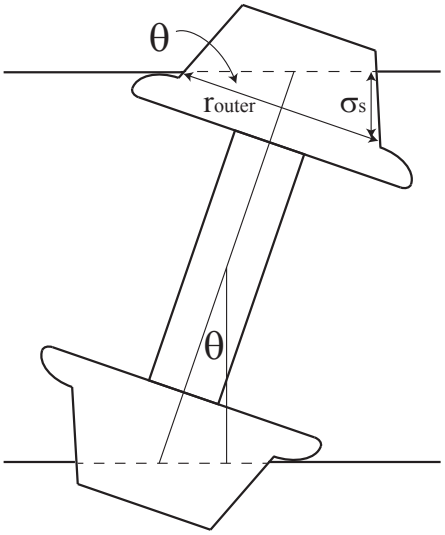

So the harmonic motion of the lateral displacement and the axle yaw have the same wavelength and different amplitudes. Furthermore, the harmonic motion of the angular deflection or axle yaw, described by a sine curve, tends to lags behind the periodic lateral displacement described by a cosine curve. This is because most track irregularities will shift the wheelset laterally and only after one wheel begins to run on a larger radius is a yaw induced. This lag between the two motions allows the wheelset system to extract energy from its forward motion up to a certain critical speed reached when the delay between angular deflection and lateral motion is a quarter cycle, as given by the initial conditions above. In other words, for a 45-degree inherent phase difference between the two cycles, the point of maximum yaw occurs as the wheelset moves through the center of the rails, defined as $y = 0$, and similarly maximum lateral displacement occurs when the wheelset is not yawed, $\theta = 0$. So this oscillation lag corresponds to the speed of the train that causes oscillations at both $y_{o_{max}}$ and $\theta_{o_{max}}$. Below the critical system speed, the lag between the two motions is less than a quarter cycle so that the motion is damped out. However, above the critical speed the lag exceeds a quarter cycle so that the lateral motion is amplified by the yaw oscillation. In the case of any greater phase difference, the oscillation magnitudes exceed the geometric constraints of the wheelset and rail, causing flange contact or derailment.

3.2 Critical Speed for the Onset of Hunting Oscillation

The critical speed for the onset of hunting oscillation can be estimated from the kinematic description of the wheelset using two methods. First, one can estimate the adhesion or frictional forces causing the motion or acceleration of the wheelset and the inertial forces that oppose this motion. Hunting oscillation occurs when the adhesion forces between the wheel and rail overcome the inertial forces opposing the oscillation, so the critical speed of onset can be found by setting the two forces equal. We will find that this estimation of the critical speed yields an overestimate of the onset of hunting. Second, the critical speed can be derived from a consideration of energy. By setting the kinetic energy of the wheelset as it rotates and translates down the track equal to the work done by the load, or weight, on the axle, we can derive a second expression for the critical speed. We will find that this estimation tends to underestimate the critical speed of the onset of hunting. Both derivations are presented in this section. The following chapter will then discuss how choices in rail, wheel, and railcar designs affect the critical speed range given by the two estimates.

3.2.1 Estimation using Inertial Forces

We define an inertial force as a force opposite in direction to an accelerating force acting on a body and equal to the product of the accelerating force and the mass of the body. For a railway vehicle running on straight track, the inertial force is the force that resists the oscillating motion of the wheelset. In order to estimate the inertial forces, we assume that the wheelset is traveling at a constant speed $V = \dfrac{x}{t}$ down the track. This provides a way to express the distance derivatives in the harmonic motion equations as time derivatives, because

$$\frac{\mathrm{d}}{\mathrm{d}\,t} = \frac{\mathrm{d}}{\mathrm{d}\,x}V$$

Then the angular acceleration of the axle in yaw can be written as

$$\frac{\mathrm{d}^2\,\theta}{\mathrm{d}\,t^2} = -V^2\left(\frac{\alpha}{rl}\right)\theta \tag{3.8}$$

where the axle is yawing about the center of the rails. We now introduce the moment of inertia of the wheelset about a perpendicular axis perpendicular through its center of mass, $I_\perp$ (see Appendix B). For any massive object, the moment of inertia is defined as the ratio of an applied torque to the angular acceleration along a principal axis of rotation. Therefore, $I_\perp$ satisfies the scalar equation:

$$\tau = I_\perp \frac{\mathrm{d}^2\,\theta}{\mathrm{d}\,t^2}$$

The inertial torque of this rotation is given by the cross product of the distance to the axis of rotation and the inertial force. Since the inertial force, F_i is acting perpendicular to the rail gauge, $2l$, we get the expression

$$\tau = (2l)F_i$$

So for the wheelset, ignoring any gyroscopic effects, we can set the two expressions for τ equal to relate inertial force and moment of inertia:

$$F_i(2l) = I_\perp \frac{\mathrm{d}^2\,\theta}{\mathrm{d}\,t^2}$$

Substituting in the angular acceleration from Equation (3.8) and solving for the inertial force yields the expression:

$$F_i = -I_\perp V^2 \left(\frac{\alpha}{2rl^2}\right)\theta$$

So we have found an expression for the inertial force counteracting the oscillation. From the mathematical expression it is clear that this inertial force is a restoring force in yaw as it follows the familiar form of Hooke's law for a spring with displacement in θ: $F(\theta) = -k\theta$, where $k = -I_\perp V^2 \left(\frac{\alpha}{2rl^2}\right)$ is a constant.

In order to estimate the critical speed, we also need an expression for the adhesion forces setting the wheelset in periodic motion. The adhesion force can be estimated as the maximum frictional force between one of the wheels and the rail:

$$F_f = \mu \frac{W}{2}$$

where W is the axle load (weight) and μ is the constant coefficient of friction between steel and steel. Generally the coefficient of friction for dry and smooth steel-to-steel contact is about 0.5 [7]. The effective friction coefficient for a rough surface could be much higher. The weight of the railcar is assumed to be evenly distributed over the two wheel-rail contacts so the load on one wheel is estimated as half of the total axle load.

Hunting occurs when the inertial forces become comparable with the adhesion forces above a certain speed that depends on the angular deflection of the axle as well as other parameters. By setting the expression for the magnitude of the inertial force equal to the expression for the frictional adhesion force, $F_i = F_f$, we can solve for the critical speed of

gross slippage:

$$I_{\perp} V^2 \left(\frac{\alpha}{2rl^2} \right) \theta = \mu \frac{W}{2}$$

$$V^2 = \mu W \frac{rl^2}{I_{\perp} \alpha} \frac{1}{\theta} \tag{3.9}$$

This expression yields a significant overestimate of the critical speed, because it assumes that there is no slippage at the wheel-rail contact and because simple limiting friction is a poor representation of the true adhesion forces. The actual adhesion forces arise from the elastic deformations of the tread and rail in the region of contact. Therefore, a complete analysis would have to take into account local creep forces, using the theory of rolling contact mechanics. These complicating considerations make the calculated sinusoidal trajectory of the wheelset, following Klingel's formula, an idealized description of the actual motion of the wheelset down straight track. However, during normal operation at lower speeds the true adhesion forces are well within the limiting friction constraint. Therefore this equation can be used as a useful first-order approximation of the upper bound on critical hunting speed.

3.2.2 Estimation using Work and Energy

We can use the fact that energy must be conserved in the kinematic solution for the hunting problem to derive another expression for the critical speed. Assuming that the railcar moves at a constant speed V down the track, we note that the oscillating motion of the railcar will continue at constant amplitude as long as the gains in energy from the forward motion of the train is exactly equal to the energy lost in work. The wheelset gains energy at zero yaw in the form of increased rotational and translational kinetic energy. The axle load, or weight on the wheelset, does work and loses energy at maximum yaw, when the load is physically lowered on one side of the rail (see Figure 3.5). In this limiting case, there is assumed to be no net energy exchange with the surroundings, so by equating the gains in kinetic energy and the losses in energy due to work at the two extremes of the oscillating system, we can estimate the critical speed.

In the previous estimation of critical speed from inertial forces, we used the tangential speed, V of the wheelset down the track to express derivatives with respect to the distance along the track, x, in terms of derivatives with respect to time, t. Similarly in this treatment, we will use the angular velocity in yaw, ω, to express derivatives with respect to time, t, in terms of derivatives with respect to the yaw angle, θ. We know that the angular velocity in

yaw is given by

$$\omega = \frac{\mathrm{d}\,\theta}{\mathrm{d}\,t}$$

This relation gives rise to the operator

$$\frac{\mathrm{d}}{\mathrm{d}\,t} = \frac{\mathrm{d}}{\mathrm{d}\,\theta}\omega$$

Using this operator and the definition of ω, the angular acceleration of the axle in yaw can be expressed as

$$\omega\frac{\mathrm{d}\,\omega}{\mathrm{d}\,\theta} = -V^2\left(\frac{\alpha}{rl}\right)\theta$$

Isolating the variables and integrating both sides of the equation, we get

$$\begin{aligned}\int \omega\,\mathrm{d}\,\omega &= -V^2\left(\frac{\alpha}{rl}\right)\int \theta\,\mathrm{d}\,\theta \\ \frac{1}{2}\omega^2 &= -\frac{1}{2}V^2\left(\frac{\alpha}{rl}\right)\theta^2 \end{aligned} \tag{3.10}$$

We know that the kinetic energy due to rotation will be of the form $KE_{rot} = \frac{1}{2}I\omega^2$. Therefore, we can introduce $I_{||}$, the moment of inertia of the wheelset along the parallel axis through its center of mass (see Appendix B), to both sides of the equation above to derive an expression for the rotational kinetic energy.

$$\mathrm{KE_{rot}} = \frac{1}{2}\mathrm{I_{||}}\omega^2 = -\frac{1}{2}\mathrm{I_{||}V^2}\left(\frac{\alpha}{\mathrm{rl}}\right)\theta^2 \tag{3.11}$$

Now that we have derived an expression for the rotational kinetic energy of the wheelset, we would like to find an expression for the change in translational energy of the wheelset as it oscillates down the track. When the wheelset is at the center of the track and both wheels are running on the same radius, r, both wheels are traveling at the same, constant tangential velocity, V. So each wheel will have a translational kinetic energy of $\frac{1}{2}mV^2$, where the individual wheel treads are considered identical in terms of mass, m (and later coning, α). So the total translational kinetic energy of the wheelset at its equilibrium position in the oscillation is given by the sum of the kinetic energies of the two wheels, so

$$\mathrm{KE_{trans_{eq}}} = \mathrm{mV^2}$$

As discussed previously, at the wheelset's point of maximum lateral displacement in the oscillation the two wheel treads are running on different radii. This means that each wheel will have a different tangential velocity (although they share an angular velocity) and

therefore each wheel will have a different kinetic energy.

We have already derived that on a curve or for a slight lateral displacement, the outer wheel runs on a radius, $r_{\text{outer}} = r + \alpha y$. So the velocity of the outer wheel will be a radial fraction of the forward velocity of the wheelset, V, defined when the wheelset is centered on the rail and both treads are running on the same radius, r. We get the expression:

$$V_{\text{outer}} = \frac{(r + \alpha y)}{r} V$$

Then the translational kinetic energy of the outer wheel is given by $\text{KE}_{\text{outer}} = \frac{1}{2}\text{mV}_{\text{outer}}^2$, so plugging in our expression for V_{outer} yields,

$$\begin{aligned} \text{KE}_{\text{outer}} &= \frac{1}{2} m \left(\frac{(r + \alpha y)}{r} V \right)^2 \\ &= \frac{1}{2} m V^2 \left(1 + 2\frac{\alpha y}{r} + \left(\frac{\alpha y}{r} \right)^2 \right) \end{aligned}$$

Similarly, for the inner wheel, we previously found that the running radius is $r_{\text{inner}} = r - \alpha y$. So the inner wheel velocity will be the radial fraction of forward velocity given by

$$V_{\text{inner}} = \frac{(r - \alpha y)}{r} V$$

Thus, the kinetic energy of the inner wheel is

$$\begin{aligned} \text{KE}_{\text{inner}} &= \frac{1}{2} m \left(\frac{(r - \alpha y)}{r} V \right)^2 \\ &= \frac{1}{2} m V^2 \left(1 - 2\frac{\alpha y}{r} + \left(\frac{\alpha y}{r} \right)^2 \right) \end{aligned}$$

So the total translational kinetic energy of the wheelset at its displaced position at zero yaw is given by the sum of the translational kinetic energies of the outer and inner wheels. So $\text{KE}_{\text{trans}_{\text{disp}}} = \text{KE}_{\text{outer}} + \text{KE}_{\text{inner}}$:

$$\begin{aligned} \text{KE}_{\text{trans}_{\text{disp}}} &= \frac{1}{2} m V^2 \left(1 + 2\frac{\alpha y}{r} + \left(\frac{\alpha y}{r} \right)^2 \right) + \frac{1}{2} m V^2 \left(1 - 2\frac{\alpha y}{r} + \left(\frac{\alpha y}{r} \right)^2 \right) \\ &= m V^2 + m \left(\frac{V \alpha y}{r} \right)^2 \end{aligned}$$

We now have expressions for the translational kinetic energy at equilibrium and the trans-

lational kinetic energy at the displaced position. So we can calculate the increase in translational kinetic energy as $\Delta\mathrm{KE}_{\mathrm{trans}} = \mathrm{KE}_{\mathrm{trans}_{\mathrm{disp}}} - \mathrm{KE}_{\mathrm{trans}_{\mathrm{eq}}}$:

$$\begin{aligned}\Delta\mathrm{KE}_{\mathrm{trans}} &= mV^2 + m\left(\frac{V\alpha y}{r}\right)^2 - mV^2 \\ &= m\left(\frac{V\alpha y}{r}\right)^2\end{aligned}$$

So to find the total kinetic energy of the oscillating wheelset system, it would be convenient to write the translational kinetic energy in terms of ω and θ. So from our earlier kinematic analysis (3.5), we found that:

$$\frac{\mathrm{d}\,\theta}{\mathrm{d}\,x} = -\left(\frac{\alpha}{rl}\right) y$$

And multiplying both sides of the equation by the velocity, $V = \dfrac{\mathrm{d}\,x}{\mathrm{d}\,t}$ we can get an expression that relates the angular velocity and the tangential velocity:

$$\begin{aligned}\frac{\mathrm{d}\,\theta}{\mathrm{d}\,x}\frac{\mathrm{d}\,x}{\mathrm{d}\,t} &= -\frac{\mathrm{d}\,x}{\mathrm{d}\,t}\left(\frac{\alpha}{rl}\right) y \\ \omega l &= -V\frac{\alpha y}{r}\end{aligned}$$

So plugging this into our expression for $\Delta\mathrm{KE}_{\mathrm{trans}}$, we are left with:

$$\begin{aligned}\Delta\mathrm{KE}_{\mathrm{trans}} &= m\left(\frac{V\alpha y}{r}\right)^2 \\ &= m(\omega l)^2\end{aligned}$$

Also noting from earlier work (Equation 3.10) that $\omega^2 = -V^2\left(\dfrac{\alpha}{rl}\right)\theta^2$, we can again substitute into our expression for $\Delta\mathrm{KE}_{\mathrm{trans}}$ to get:

$$\begin{aligned}\Delta\mathrm{KE}_{\mathrm{trans}} &= ml^2\omega^2 \\ &= -ml^2V^2\left(\frac{\alpha}{rl}\right)\theta^2 \qquad (3.12)\end{aligned}$$

We want to find the total energy extracted from the forward motion of the wheelset as it oscillates down the track. This total energy is given by the rotational kinetic energy of the wheelset (3.11) plus the increase in translational kinetic energy (3.12). So the total kinetic

energy of the oscillating wheelset system is given by $\mathrm{KE}_{\mathrm{total}} = \mathrm{KE}_{\mathrm{rot}} + \Delta\mathrm{KE}_{\mathrm{trans}}$:

$$\begin{aligned}\mathrm{KE}_{\mathrm{total}} &= -\frac{1}{2}I_{||}V^2\left(\frac{\alpha}{rl}\right)\theta^2 - ml^2V^2\left(\frac{\alpha}{rl}\right)\theta^2 \\ &= -\frac{1}{2}V^2\left(\frac{\alpha}{rl}\right)\theta^2\left[I_{||} + 2ml^2\right] \end{aligned} \tag{3.13}$$

Now that we have derived an expression for the total kinetic energy gained at zero yaw, we would like to estimate the energy loss of the system due to the weight of the wheelset (and attached railcar). In our model, this lost energy is equivalent to the work done by the axle load when the wheelset is at maximum yaw. To understand how the load on the axle does work we need to more precisely quantify how the axle moves in space. Until now, we have been considering only the lateral movements of the wheelset center and yaw. However, when the axle yaws and the points of contact between wheelset and rail move in relation to the coned treads, the difference in radii also causes a change in the vertical height of the wheelset above the rail. To calculate the change in vertical height of the wheelset, we can use the conicity of the tread and the change in distance between the support points caused by the yaw. First, from Figure 3.5 we see that at the maximum yaw of θ, the distance between the inner and outer contact points increases to:

$$d = \frac{2l}{cos(\theta)}$$

Figure 3.5: Increased distance between wheel-rail contacts for a wheelset at maximum yaw.

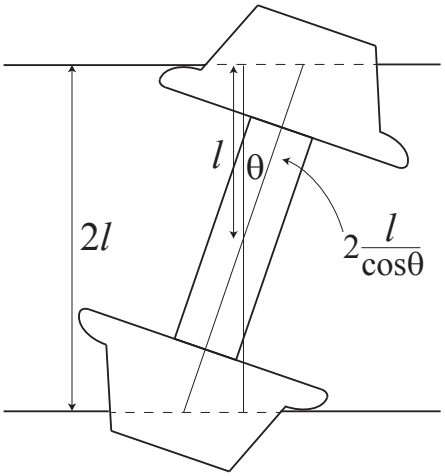

Using the second-order truncation of the Taylor series expansion: $\sec\theta \approx 1 + \frac{1}{2}\theta^2$ in the limit that $\theta \to 0$ (more commonly known as the small-angle approximation), we can rewrite

this increased distance as:

$$d \approx 2l\left(1+\frac{1}{2}\theta^2\right) \approx 2l + l\theta^2$$

Then we can find an expression for the displacement of the support point from the center of the tread for one of the wheels:

$$\Delta d = \frac{1}{2}\left(d - 2l\right) = \frac{1}{2}\left(2l + l\theta^2 - 2l\right) = \frac{1}{2}l\theta^2$$

Then the axle load falls by a height proportional to the displacement of the contact points on the coned tread (see Figure 3.6):

$$\Delta h = \alpha \Delta d = \frac{1}{2}\alpha l\theta^2$$

Figure 3.6: Change in axle height with maximum yaw.

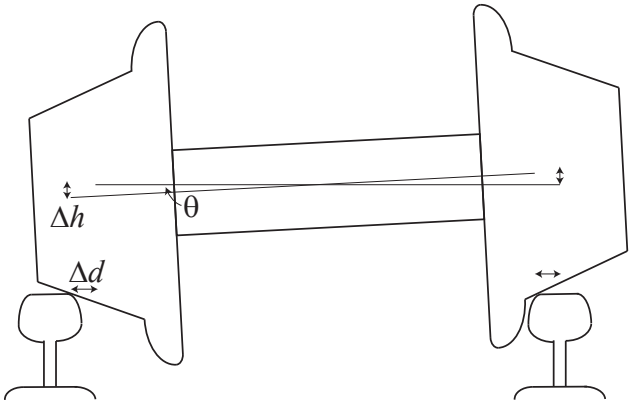

Then the work done by the weight of the wheelset and railcar, W, in lowering the axle load a distance Δh is given by $\mathrm{W_{load}} = \mathrm{W}(\Delta \mathrm{h})$:

$$\mathrm{W_{load}} = \frac{1}{2}\mathrm{W}\alpha l\theta^2 \tag{3.14}$$

The work done by the axle load is the energy lost from the system. In order for the motion of the wheelset to continue, at least an equal amount of energy must be extracted from the forward motion of the wheelset since energy is conserved. So the critical speed is found from the energy balance; in other words, the critical speed occurs where the magnitude of the total kinetic energy of the oscillating wheelset (3.13) equals the work done by the axle

load (3.14). Setting $\mathrm{KE}_{\mathrm{total}} = \mathrm{W}_{\mathrm{load}}$ and solving for V yields the expression:

$$\begin{aligned} \frac{1}{2}V^2\left(\frac{\alpha}{rl}\right)\theta^2\left[I_{||}+2ml^2\right] &= \frac{1}{2}W\alpha l\theta^2 \\ V^2\frac{\left[I_{||}+2ml^2\right]}{rl} &= Wl \\ V^2 &= \frac{Wrl^2}{I_{||}+2ml^2} \end{aligned} \tag{3.15}$$

This estimation for the maximum or critical speed on straight track is independent of the wheel taper, but depends on the ratio of the axle load to wheel set mass. If the treads were truly conical, independence from α would hold as described. However, in practice wear on the wheels cause the taper to vary across the tread width, so that the value of the taper used to determine the energy lost (or work done by the axle load) is different from that used to calculate the kinetic energy gained; so they do not cancel out. Denoting the conicity of the kinetic energy as k and the conicity of the work done as α, we get a more general critical speed equation of:

$$V^2 = \frac{W\alpha rl^2}{k[I_{||}+2ml^2]} \tag{3.16}$$

where α and k are now shape factors determined by the wheel wear. This generalized result is derived in [25] from an analysis of the system dynamics using standard control engineering methods.

We previously hinted that this expression for the critical speed of the onset of hunting oscillation is an underestimate of the true onset speed. This is mainly due to two assumption of the kinematic model: the first being that the energy of the system is conserved and the second being that we consider only a single wheelset, devoid of any suspension systems or coupling to other axles in a truck. We modeled the energy lost at maximum yaw as simply the work done by the lowering of the axle load, or weight. However there are many other sources of energy loss when one considers deformations of the wheel and rail and heat and sound energy dissipated to the surroundings. If the assumption of energy conservation were relaxed and we could quantify these additional losses, the speed given by Equation (3.15) would be much higher. Furthermore, the energy loss term can also be increased by considering the wheelset as a part of a larger truck and suspension system. By including an elastic constraint on the yaw motion of the axle, we can introduce an additional energy loss arising from spring tension or elastic forces. This motivated the arrangement of wheelsets in suspension frames, or bogies, to increase the constraint on the yaw motion of the wheelsets

and to apply elastic constraints, ultimately to raise the maximum allowable speed (before the onset of hunting).

It should be noted that the motion of a wheelset itself is more complicated than the simple periodic motion analysis would indicate, especially when considering the many components that couple the wheelset to the railcar. For example, the vehicle suspension applies additional restraining forces so that at high speed, the wheelset generates additional gyroscopic torques. These additional torques will modify the estimate of the critical speed. Furthermore, a real railway vehicle has many more degrees of freedom than an individual wheelset and, consequently, may have more than one critical speed; and it is by no means certain that the lowest speed is dictated by the wheelset motion derived above.

Although the critical speed estimate from purely kinematic consideration is not exact, the analysis is instructive because it shows why hunting oscillation, a very real and important aspect of railway motion, occurs. We have shown that as the speed increases, the inertial forces become comparable with the adhesion forces. This is why the critical speed depends on the ratio of the axle load (which determines the adhesion forces) to the wheelset mass and geometry (which determine the inertial forces). From these kinematic equations we can also see that below a certain speed, the energy which is extracted from the forward motion of the train is insufficient to replace the energy lost by lowering the axles. In this situation, the periodic motion damps out and the wheelset eventually returns to its central position along the track, assuming there is no further perturbation. However, above this critical speed, the energy extracted by the forward motion is greater than the loss in energy and the amplitude of oscillation builds up. In this case, only shortly after the onset of hunting, the amplitude of oscillation will exceed the maximum possible lateral displacement constrained by the standard play. The wheel flanges will impact the rails, potentially causing damage to both the wheel and track, and in more serious cases causing sufficient lateral forces for the wheel to mount the rail, derailing the car. The following chapter will use the critical speed equations derived from kinematic approximations to explore how track and wheelset geometric design as well as railcar loading influence hunting oscillation and the maximum speed it imposes.

3.3 Other Straight Track Derailments

This chapter has focused on the description of wheelset hunting, or the oscillation of lateral displacement and yaw of a wheelset down tangent track. It is also important to note that there are other dynamics that can cause derailment on these same sections of track. The

two most prevalent of these other instabilities, bounce and harmonic roll or rock-off, take into account dynamics not just on the wheelset, but also on the railcar.

3.3.1 Bounce

Bounce refers to the vertical motion of a vehicle. Freight cars sit on two trucks, one on each end, that supports the wheels, axles, and bearings. The standard truck consists of two side frames with a bolster mounted on a spring in the middle. A train traveling on bumpy track will bounce the freight car body up and down on the spring-mounted bolster [8]. Bounce is induced by any number of factors, including rail and track defects, going from a section of relatively soft roadbed to stiff roadbed (such as at a grade crossing or bridge abutment), or excessive speed. In general, vertical perturbations from track dips and other factors are resisted by the friction wedges of the railcar which act like shock absorbers in an automobile. If these friction wedges wear out or the car bounces too energetically, it causes weight transfer among the wheels that can result in wheel climb. In severe cases, the weight on the wheel is reduced (and the L/V ratio is increased) to the point that the wheel lifts completely off the rail. Bounce usually occurs at speeds above 40 mph [16].

3.3.2 Harmonic Roll

Harmonic roll refers to the side-to-side, resonant rocking motion of a railcar body. It most often occurs on jointed track where the spacing of the trucks closely matches the spacing of the joints [16]. This is because the rail joint is one of the weakest points of the track and can flex and cause the wheel to dip. Since rail joints are staggered, the wheels dip on one side and then the other causing the car to rock back and forth [8]. Other factors such as a shifting load, high center of gravity, or damaged or missing car suspension components can also cause or contribute to harmonic roll. If the motion magnifies or resonates, wheel lift or wheel climb results because the vertical load on one wheel is lessened or in some cases is negative (upward) [16]. Derailments caused by harmonic roll usually require several cycles of roll before the forces and conditions are sufficient to cause the derailment. Furthermore, like the case of a heavy and tall railcar on a highly banked curve, harmonic rock-off derailments usually occur at low speeds, particularly between 10 and 25 mph [16]. Therefore, harmonic roll is more problematic for freight vehicles that are also more likely to have higher centers of gravity.

Chapter 4

Parametric Analysis for Speed on Straight Track

4.1 Lateral Displacement and Axle Yaw Oscillation

In the previous chapter we demonstrated that, if perturbed from a straight path, the coned wheelset on straight track oscillates in both lateral position and axle yaw. We found that these displacements are described, to a first approximation, as simple harmonic motion with lateral displacement following Equation (3.1) and axle yaw, which lags behind lateral displacement by a quarter of a cycle, following Equation (3.6):

$$y = y_o \cos\left(\frac{2\pi}{\lambda}x\right)$$

$$\theta = \theta_o \sin\left(\frac{2\pi}{\lambda}x\right)$$

We found that the maximum amplitude of the lateral oscillation, $y_{o_{max}}$, is constrained by half of this standard play between the wheelset and the rails according to Equation (3.3):

$$y_{o_{max}} = l - \frac{w}{2} - t$$

and that the maximum yaw of the wheelset is related to $y_{o_{max}}$ by Equation (3.7):

$$\theta_{o_{max}} = \sin^{-1}\left(\frac{2y_{o_{max}}}{r + \alpha y_{o_{max}}}\right)$$

We also noted that both the lateral displacement and axle yaw oscillations had the same periodicity, with wavelength given by Equation (3.2) and frequency given by Equation (3.4):

$$\lambda = 2\pi\sqrt{\frac{rl}{\alpha}}$$

$$f = \frac{V}{2\pi}\sqrt{\frac{\alpha}{rl}}$$

From these equations for the periodic motion of the wheelset down tangent track, it is clear that the lateral displacement and axle yaw oscillations depend on the gauge of the track, $2l$, and a number of geometric factors of the wheelset. For example, the oscillation amplitude depends on the axle width, w, and the flange thickness, t, while the wavelength of the oscillation depends on the average running radius of the wheels, r, and the conicity of the treads, α. The following sections explore how some of these track and wheelset geometries affect the lateral displacement and axle yaw oscillations for a hunting railcar. Later in the chapter, we will explore how the critical speed of he onset of these hunting oscillations is also affected by many of these same geometries, as well as railcar loading.

4.1.1 Rail Gauge

The US railroad network is constructed almost exclusively with 56.5 inch standard gauge. As previously mentioned, this gauge is maintained to strict tolerance levels because constant use or faulty installation can narrow or widen gauge, which can affect the dynamics of wheelsets and railcars on both curved and straight track. We have seen that narrowed gauge can exert sufficient lateral forces on a wheel to cause it to climb the rail. Although this is more common in curving situations, the same problem can arise during hunting oscillation, when one wheel adopts a more lateral position than the other. However, on tangent track a more common gauge problem is wide gauge, which can increase hunting and cause rough riding [16].

From the derived oscillation equations, it is clear that the rail gauge, $2l$, factors into the wavelength of both the lateral displacement and axle yaw oscillations. It also appears in the calculation of standard play, which constrains the maximum amplitudes of these oscillations. For a standard gauge wheelset, wider gauge leads to a longer wavelength (lower frequency) but a higher amplitude of oscillation. Although lower frequencies of oscillation are often desirable, the increase in oscillation amplitude with widened gauge is what causes rough riding. Since the maximum lateral acceleration of the wheelset in oscillation is related to the amplitude of that oscillation, this increased amplitude means that the laterally-oscillating

wheelset exerts greater force on the rails as it travels back and forth along the track. These more forceful oscillations can cause increased damage to wheel and rail, lead to instabilities, and can be felt more severely by passengers or delicate freight. Therefore, for the standard North American interchange freight wheel, AAR1B, a maximum of 1.2 inches of gauge widening from the standard value is allowed for a freight vehicle operating in the low-speed range of 25 to 40 mph [28]. For higher-speed, lighter passenger trains, rail gauge widening is even more strictly maintained.

Other Gauge Systems

Although the majority of railroad lines in America and many new lines abroad are constructed with standard gauge, we have seen that around the world here exist narrow and broad gauge systems. These systems have significantly different dynamic oscillations on tangent sections of track. In general, narrow gauge results in a lower wavelength (higher frequency) of oscillation while a broad gauge results in a higher wavelength (see Figure 4.1).

Figure 4.1: Lateral oscillation for new wheelsets on narrow, standard, and broad rail gauge systems.

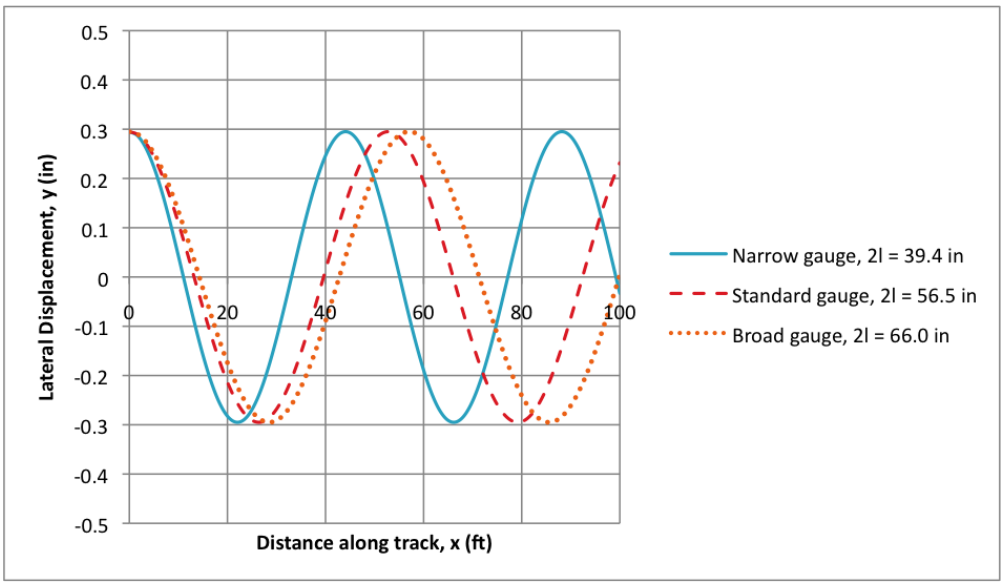

Although the periodicity of oscillation varies across gauge systems, there is little difference in oscillation amplitudes on narrow, standard, and broad gauge. This is because in industrial practice, most wheelsets are constructed so that the standard play is comparable on narrow, standard, and broad gauge. In other words, wheelsets made for narrow gauge lines have

proportionally smaller axle widths and flange thicknesses. Similarly, wheelsets constructed for broad gauge lines have larger axle widths and thicker flanges. Therefore, although the rail gauge appears in the calculation for oscillation amplitude, system-specific construction of wheelsets practically eliminates the affect of gauge on amplitude.

Since broad gauge systems then have lower oscillation frequencies at roughly the same amplitude, broad gauge is desirable for most rail traffic. In the next section, we will see that broad gauge also leads to higher onset speeds of straight track instabilities. This means that broad gauge construction contributes to riding comfort and increases maximum speed limits on tangent track. Despite this fact, broad gauge is not generally used for lighter, faster passenger lines because of its more expensive, solid construction. For this reason, broad gauge is still used mostly for heavy, slow freight traffic.

In industrial practice the gauge of the track can be regularly maintained so that it conforms to strict tolerance levels even under heavy usage. This means that prompt, although costly maintenance can help reduce if not eliminate many of the instabilities due to oscillation on straight track. Irregular gauge can also cause irregular rail head wear, which in turn degrades the alignment and surface of the tracks. Therefore, maintaining rail gauge also helps reduce wheel wear, which is another important focus of rail maintenance. This wheelset wear, not unrelated to misalignment of track, will be explored more extensively in the next section.

4.1.2 Wheel Geometries: Flange Thickness and Conicity

As trains run in service, uneven wear on the flange and wheel treads can cause substantial changes in wheelset geometries. If a train takes curves too quickly and forces flange contact or oscillates on straight track, over time the thickness of the flange will decrease. Worn or defective wheel flanges can cause or contribute to a train derailment. In some cases, flanges become sufficiently thin to allow a wheel to drop between the rails. Flange wear also increases the play between the wheel and rail and therefore increases the maximum allowable amplitude of lateral oscillation. This more severe hunting can lead to increased lateral wheel rail forces, possibly causing wheel climb.

If we consider the standard North American freight wheel profile, the AAR1B, on standard gauge of $2l = 56.5$ inches, new wheelsets are constructed with an axle width of $w = 53.15$ inches and a flange thickness of $t = 1.38$ inches per wheel [28]. These newly manufactured geometries give the wheelset a standard play of $\sigma_s = 0.59$ inches and a corresponding maximum oscillation amplitude of $y_o = 0.295$ inches, also called the flangeway clearance. This agrees with industrial values which state an average flangeway clearance of $0.28 - 0.39$ inches

[26].

In service, however, running with flange contact wears the wheels and reduces the flange thickness. Since a maximum of 0.59 inches of flange wear is allowed before wheelsets must be decommissioned or re-profiled, a completely worn-out wheel can have a flange thickness of as little as 0.79 inches [28]. Although this is the extreme value, most wheel flanges with thickness of 15/16 (or 0.947) inch or less are considered condemnable [16]. This smaller flange thickness, given no change in the rail or wheel gauge, yields a much higher standard play of 1.77 inches. This corresponds to a flangeway clearance of 0.885 inches, more than doubling the upper limit on the oscillation amplitude for a newly manufactured wheel (see Table 4.1). So for a new wheelset and rails, the maximum yaw is only about 2 degrees and the maximum lateral displacement is 0.3 inches. At the geometric limits of wear before cancelation of service, the value of the maximum yaw and the maximum lateral displacement triples, to a values of a little under 6 degrees and 0.9 inches respectively.

Table 4.1: Amplitude and wavelength of wheelset oscillation for new and worn AAR1B wheel of running radius $r = 18$ inches on standard gauge.

	Flange Thickness, t (in)	Conicity, α	Amplitude, y_o (in)	Wavelength, λ (ft)
New Wheel	1.38	0.5	0.295	53
Worn Wheel	0.79	0.35	0.885	20

Wear affects not only the flange, but also the profile of the tread of the wheel, thereby affecting the wheel-rail interface and potentially increasing the likelihood of a derailment [16]. The other wheelset geometry most noticeably affected in service is the tread conicity, or the slope between the outer and inner wheel tread radii. For new wheels, the conicity is manufactured at a value of 1/20 or 0.05 for most railways. In service, however, the value of the effective tread conicity increases with wear (Figure 4.2).

Figure 4.2: Effective conicity of a worn wheel profile.

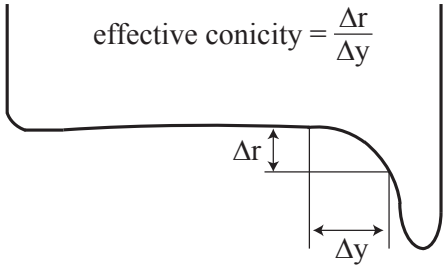

This increase in conicity over time decreases the wavelength of the kinematic oscillations. In fact, railroad standards allow a wheel with conicity up to 0.35 to remain in service [27]. Holding all other variables constant, this increase in conicity with wheel wear can change the wavelength of oscillation from 53 feet to as little as 20 feet (see Table 4.1). This decreased wavelength means more frequent back and forth oscillation of the train along the track, which can add additional lateral stress to the rails and make for a less comfortable ride.

Considering the wear effects on wheel geometries simultaneously, we see that decreased flange thickness increases the amplitude of oscillation while increased conicity decreases the wavelength of oscillation. These wear effects sum to give much more rapid and violent oscillations in lateral displacement and axle yaw for wheelsets that have seen significant service (see Figures 4.3 and 4.4). The following section explores how the more rapid frequency of oscillation affects passenger comfort (as well as the state of more delicate freight).

Figure 4.3: Lateral displacement oscillations for new and worn-out wheelsets.

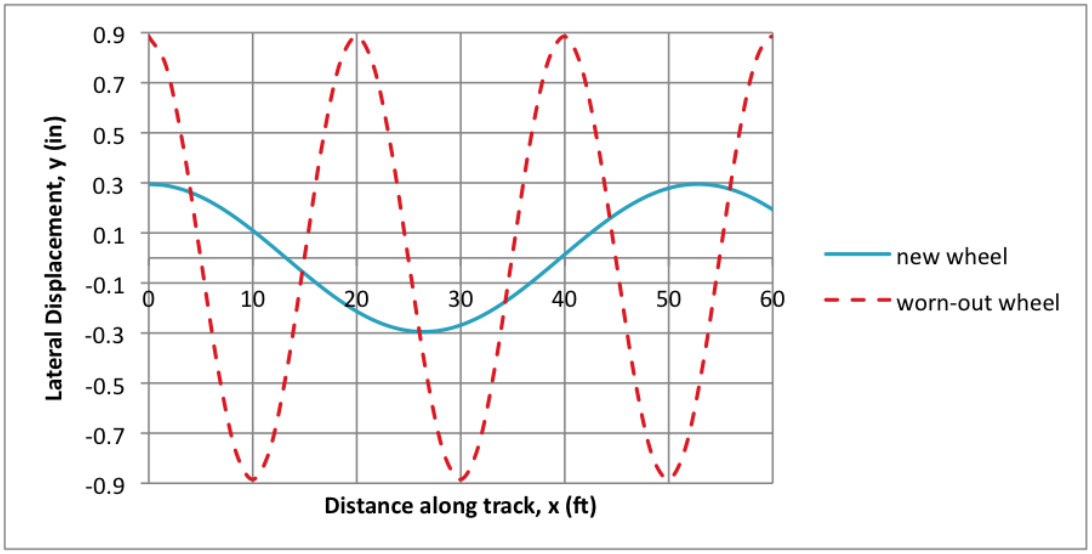

Figure 4.4: Axle yaw oscillation for new and worn-out wheelsets.

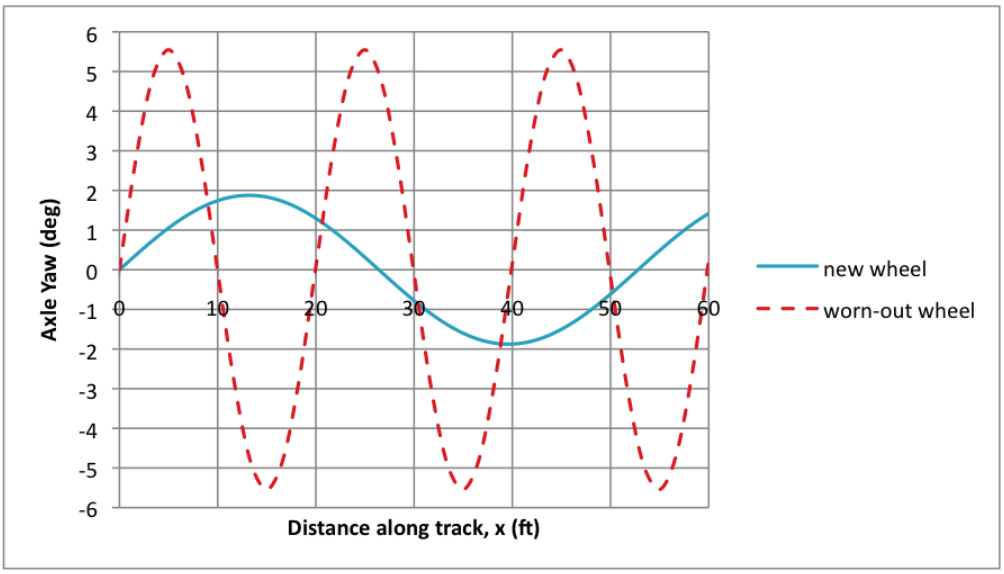

4.2 Riding Comfort

We have seen how changes in rail and wheelset geometries affect the oscillatory motion, particularly the wavelength, of the railcar on tangent track. Another way of characterizing the periodicity of the oscillation is by looking at frequency rather than wavelength. In the previous chapter, we derived Equation (3.4) for the frequency of both the lateral displacement and axle yaw oscillations:

$$f = \frac{V}{2\pi}\sqrt{\frac{\alpha}{rl}}$$

This frequency depends most heavily on the constant longitudinal speed, V, of the train down the track, but is also related to the same wheel and rail geometries that affect wavelength. Examining how these parameters affect the frequency of hunting oscillation is important because vibrations in the railcar can be unpleasant for passengers. Therefore, measuring the mechanical or physical vibrations can serve as a way to quantify passenger comfort, which is also affected by more subjective environmental factors such as noise level, temperature, and humidity [18].

Today one main standard for assessment of whole-body vibration exposure is ISO 2631 [1]. However, this standard is not a perfect quantification of rail passenger comfort because it is not specific to railroad vehicles which often exhibit different vibrations than other forms of transport. The vibrations in railroad vehicles are unique because passengers experience

low overall acceleration magnitudes, because the vibrations fluctuate due to train speed and variations in track quality, and because the peak frequencies are linked to the particular suspension characteristics of the railway bogie [18].

Investigations have shown that the human body is most sensitive to vibrations in the frequency range of 4 to 6 Hz (although some sensitivity remains frequencies of up to 30 Hz). A newly constructed railcar with fully-functioning suspension system generally has vibrations in the frequency range of 0.5 to 2 Hz [18]. This is somewhat lower than the vibrations that cause the most discomfort to passengers, so that overall vibrations in trains are not sever. However, any defects in the railcar or wheelset that cause an increase in oscillation frequency can potentially impact passenger comfort. It has been found that, in a railcar, the greatest resonance peaks are in the transverse and vertical directions, where the transverse frequencies are related to the hunting of the wheelset and the vertical frequencies are linked to the suspension characteristics of the railway vehicle [18]. It has been found that the vibration acceleration value is higher near the seat and these vibrations are transmitted along mainly the vertical direction. This is why back pain is the most common complaint of rail passengers [29]. Furthermore, due to its length, the body of the railway carriage is not rigid and a modern steel railway vehicle may have a resonant frequency of 8 Hz or above in the longitudinal direction.

There are several standardized methods of measurement and assessment of whole-body vibration in moving trains specifically. One of the first attempts to provide a metric which correlates objective vibration measurement to the subjective parameter of ride comfort (or quality) was proposed by Sperling. Dr. Sperling found that depending upon the frequency range, the sensitiveness of the human body is related to acceleration to which it is subjected. Under Sperling's comfort index system, which is still used today, the vehicle is assessed according to the effect of mechanical vibration on the occupant according to the equation [18] [29]:

$$W_z = \left(\sum_{i=1}^{n_f} W_{z_i}^{10} \right)^{1/10} \tag{4.1}$$

where n_f is the total number of discrete frequencies of the acceleration response of the railway vehicle identified by Fourier analysis and W_{z_i} is the comfort index corresponding to the i^{th} discrete frequency, f_i in Hz. Each W_{z_i} is given by:

$$W_{z_i} = \left(a_i B(f_i^2) \right)^{3/10} \tag{4.2}$$

where a_i denotes the amplitude of the peak acceleration in m/s^2 of the i^{th} and $B(f_i)$ is a derived frequency dependent weighting factor that expresses human vibration sensitivity. This weighting factor for a given frequency is:

$$B(f) = k\sqrt{\frac{1.911f^2 + (0.25f^2)^2}{(1 - 0.277f^2)^2 + (1.563f - 0.0368f^3)^2}} \tag{4.3}$$

where the coefficient k is different for vertical (equal to 0.588) and horizontal (equal to 0.737) vibration components [14]. The index number given by Equations (2.1), (2.2), and (2.3) for the frequency distribution in a railcar is then correlated to a subjective measurements of riding comfort given in Table 4.2 [18] [14].

Table 4.2: Numerical values for various degrees of riding comfort.

Index	Subjective Ride Comfort	Body Fatigue Onset
1.0	Very good; barely noticeable	
1.5	Almost good	over 24 hours
2.0	Good, but noticeable	
2.5	Nearly good; more pronounced but not unpleasant	10.0 hours
3.0	Passable; strong, irregular but still tolerable	5.0 hours
3.5	Extremely irregular and unpleasant, prolonged exposure intolerable	2.8 hours
4.0	Able to run, but extremely unpleasant, prolonged exposure harmful	1.5 hours
4.5+	Not able to run; dangerous	45 minutes or less

The kinematic analysis derived in the previous chapter does not take into account the suspension characteristics of the railcar, so it cannot present a complete picture of passenger riding comfort. From Equation (3.4), it is clear that the faster the train is moving, the higher the frequency of hunting oscillation and therefore the more likely that these frequencies will be within the range of human discomfort. The frequency of the oscillation in the railcar also changes if the conicity is changed. Therefore, some high speed passenger rail routes have adopted a conicity of 1/40 instead of the standard 1/20. However, this change in conicity, if not accompanied by changes in track design, can cause unstable and uncomfortable resonance between the vehicle and the track.

More sophisticated computer simulations, such as the one performed in [18], can shed light on how frequency and riding comfort related to speed and other parameters (see Figure 4.5). From Figure 4.5, it is clear that the Sperling's ride index value can be quite high for freight trains, reaching up to 2.8 for a subjective ride comfort between "More pronounced

but not unpleasant and "Strong, irregular but still tolerable [18]. This is not necessarily a concern for most freight traffic, although can be a problem for the transport of fragile goods and can potentially affect the alertness of the engineer and crew. For the passenger train, the Sperling's ride index maximum value is 2.2 and this means that the subjective ride comfort is found between "Clearly noticeable and "More pronounced but not unpleasant.

Figure 4.5: Simulated Sperling's ride index for a freight train (△) and a passenger train (◯) traveling at various speeds.

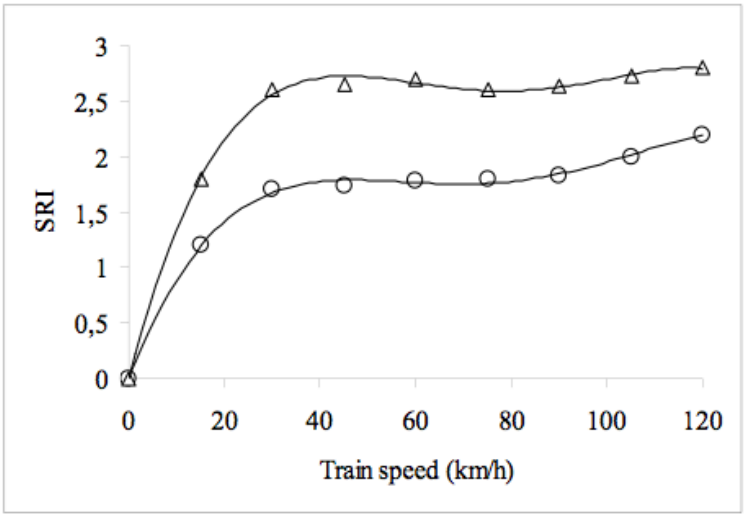

We conclude that it is evident that ride index as an evaluation criterion is exclusively based on the comfort consideration of the passengers traveling in the coach. This is an important parameter to consider when designing suspensions for passenger cars, but to apply this criterion for the assessment of the safety of operation of general rolling stock would be too rigid a standard. Instead, safety standards should be based on running speeds at which these oscillations are damped out and do not cause risk of derailment from amplification.

4.3 Critical Speed of the Onset of Hunting

The previous section explored how rail and wheel geometries affect the unstable periodic motion of the hunting wheelset down tangent track. In this section we will explore how some of these same parameters affect the critical speed at which these oscillations are amplified. Because hunting is a serious safety concern, the critical speed of oscillation onset is effectively a maximum operation speed. In Chapter 3, we derived the critical speed for the onset of hunting oscillation using two different methods: (1) estimation of inertial and frictional forces, and (2) considerations of work and energy. We noted that Equation (3.9) for the

critical speed of hunting oscillation derived from (1) was likely an overestimate due to limiting assumption of simple friction as the adhesion force:

$$V^2 = \mu W \frac{rl^2}{I_\perp \alpha} \frac{1}{\theta}$$

We also argued that Equation (3.15) derived from (2) was likely an underestimate due to the limiting assumption of energy conservation:

$$V^2 = \frac{Wrl^2}{I_{||} + 2ml^2}$$

In the following parametric analysis, we will use these two equations to give an upper and lower bound for the critical speed of hunting oscillation onset. We find that these equations do indeed bound published experimental or simulated values for different rolling stock and rail characteristics. We will use this analysis to discuss the implications for rail and railcar design as well as maintenance of straight track.

4.3.1 Railcar Weight and Wheel-Rail Geometries

The American Association of Railroads (AAR) sets interchange rules on freight car capacities on US rail lies. The AAR defines and regulates a number of different types of car empty and loaded weights. The gross rail load is defined as the maximum permissible weight of a loaded freight car in interchange service based on the size of the wheel axle used [3]. The tare or empty weight of a car rounded to the nearest 100 pounds is known as the light weight. From the gross rail load and the light weight, the AAR defines the load limit or the maximum amount of lading by weight that can be carried by a specific car. The load limit is the difference between the gross rail load and the light weight, expressed to the nearest 100 pounds. Finally, the AAR defines a car's capacity as the nominal amount of lading a car can carry in 1000 pounds. The car capacity can be no more than the load limit [3]. In general, freight cars are classified according to nominal carrying capacity from 30-125 tons. On the US network, 100-ton capacity cars with 4 or 6 axles are the most common [16]. Table 4.3 modified from Rule 89 of the Field Manual of the AAR Interchange Rules, gives the maximum weight on the rails allowed for certain freight car dimensions as well as the nominal capacity while Table 4.4 gives the light weight ranges for different types of freight cars.

Because most passenger-carrying systems do not engage in interchange service, passenger car design, operation, and performance tend to be more specialized to a particular network

Table 4.3: Gross weight limits for freight cars of certain dimensions.

Journal Size	4-axle (lb)	6-axle (lb)	Nominal Capacity (T)	Wheel Diameter (in)
$4\frac{1}{4} \times 8$	103,000	154,500	—	—
5×9	142,000	213,000	—	—
$5\frac{1}{2} \times 10$	177,000	265,500	50	33
6×11	220,000	330,000	70	33
$6\frac{1}{2} \times 12$	263,000	394,500	100	36
$6\frac{1}{2} \times 12$	286,000	429,000	100	36
7×12	315,000	472,500	125	38

Table 4.4: Light weights of various types of freight cars.

Car Type	Light Weight (T)
Boxcar	29-47
Refrigerator car	42-51
Flat car	29-41
Gondola car	33-39
Hopper car (open top)	25-32
Hopper car (covered)	21-35
Tank car	28-55

and therefore vary greatly from system to system. All passenger cars are generally designed and maintained to the specifications of AAR Standard S-034.49 C.F.R. 238 [16]. Amtrak cars include baggage, sleeper, dormitory, coach, lounge, dining, mail, and other types of cars. Table 4.5 shows the wide variety of dimensions and weights for Amtrak passenger cars of different types [16]. Amtrak trains usually consist of one or two locomotives with anywhere from four to twenty-two cars of various types [11].

From Equations (3.9) and (3.15) for both the upper and lower bounds on the maximum speed of the onset of hunting oscillation, it is clear that one of the most important parameters in straight track stability is the weight on each wheelset or the axle load, W. In general, the higher the axle load the higher the critical speed before the onset of hunting. This is because the higher the magnitude of the axle load, the greater the frictional forces between the wheel and rail. These higher frictional forces counteract the inertial forces or lead to greater energy loss (see Table 4.6).

Because hunting oscillation does not occur for heavy trains until very high speeds, most freight traffic is protected from these straight track instabilities. This is because freight cars tend to be heavier and to already move at slower speeds. Therefore, this means that if a car in a freight trains does experience hunting oscillation, it is often an empty car being

Table 4.5: Dimensions and weights for various types of Amtrak cars.

Series	Type	Length (ft)	Light Weight (lbs)	Capacity (1000 lbs)
Heritage	Dormitory	85	126,500	10
	Lounge	85	161,600	86
Amfleet I	Amcoach	85	106,000	78
Amfleet II	Amlounge	85	109,600	49
Viewliner	Sleeper	85	136,000	30
Superliner I	Coach	85	147,500	62
	Sleeper	85	155,700	44
—	Baggage	74	96,400	—
—	Mail	64	92,400	—

Table 4.6: Calculated upper and lower bounds on the critical speed of hunting oscillation for representative 6-axle freight and passenger cars with 36-in wheels.

		V_{critical}	
		Lower Bound (mph)	Upper Bound (mph)
Freight Boxcar	$W_{\text{empty}} = 120000$ lbs	11	178
	$W_{\text{gross}} = 65750$ lbs	26	416
Passenger Coach	$W_{\text{empty}} = 17667$ lbs	14	215
	$W_{\text{gross}} = 30667$ lbs	18	284

transported to another part of the network. We have discussed previously how not all cars in a freight train are loaded and how an uneven distribution of empty and loaded cars can have some effect on the train's dynamic behavior. Discussion of slack effects on curves stressed the importance of managing the location of empty cars due to their lower L/V ratios and higher chance of derailment. This analysis of straight track reinforces the importance of trying to load cars evenly and keeping the empty cars to the back of the train, since they are the most likely to exhibit unstable oscillation on stretches of tangent track.

Truck-hunting is particularly severe for high-speed passenger trains that also tend to be lighter than their laden freight counterparts. As a result, limiting hunting oscillation presents a critical design concern for passenger rail lines. Most passenger equipment today is designed for operating speeds of at least 110 mph, which for the lighter-weight vehicles can be dangerously close to the critical speed for the onset of hunting instability given by the derived kinematic equations. For this reason all cars on all trains operating above 125 mph in the United States have sensors that sound an alarm if truck-hunting occurs [8]. For many years, classic hunting oscillation limited steel-wheeled trains to operation speeds of about 140 mph (for heavy cars). The design of new suspension systems, which are neglected in the

kinematic derivations, have more recently permitted speeds exceeding 180 mph [26].

The consideration of axle load as a major factor determining the maximum safe operating speed on tangent track becomes particularly important when one realizes that the other parameters in the equation for the critical hunting speed, such as wheel tread radius, coning and rail gauge, are not usually considered variables in the design of railcars and straight track sections. The following two short sections look at how discrete industry values of wheel diameter and rail gauge affect the maximum speed equation at varying values of axle load.

Wheel Diameter

Diesel-electric locomotives are generally equipped with 40 or 42-inch wheels. Wheel sizes for freight cars vary with the type of rolling stock, but generally have values of 33, 36 (most common), or 38 inches (see Table 4.3). Mainline passenger cars typically also have 36-inch wheels although some commuter lines use diameters as low as 28 inches [16]. The affect of these different wheelset radii on the onset speed of hunting oscillation is not immediately obvious, since radius appears both in the numerator and in the denominator (in the moments of inertia of the wheelset) of both the upper and lower bound critical speed equations. We find that the numerator relationship dominates so that larger wheel diameters allow higher speeds before the onset of instability (see Figures 4.6 and 4.7).

Figure 4.6: Upper bound on the critical speed of hunting oscillation as a function of axle load for wheels of different average wheel diameters.

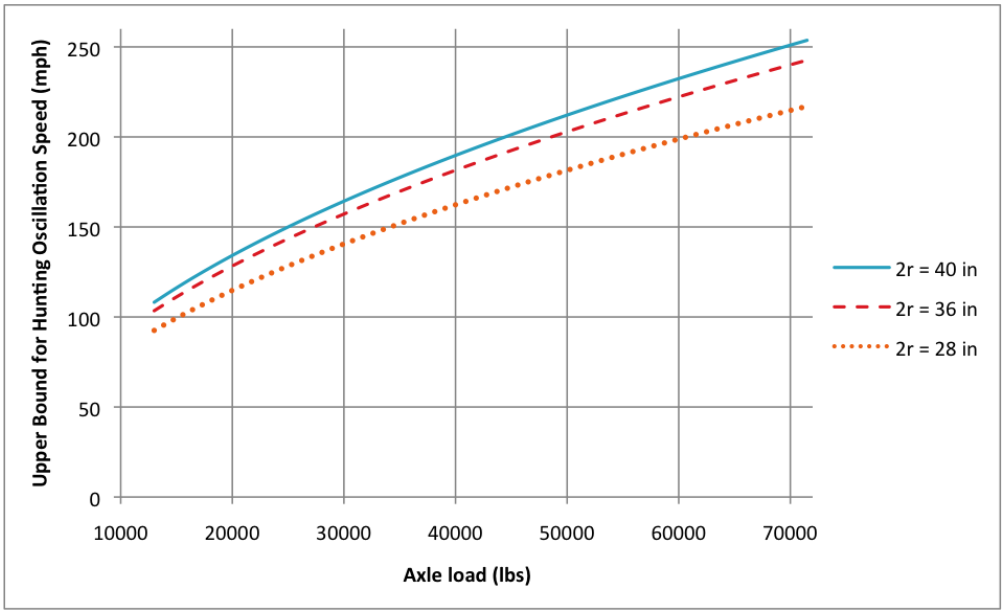

Figure 4.7: Lower bound on the critical speed of hunting oscillation as a function of axle load for wheels of different average wheel diameters.

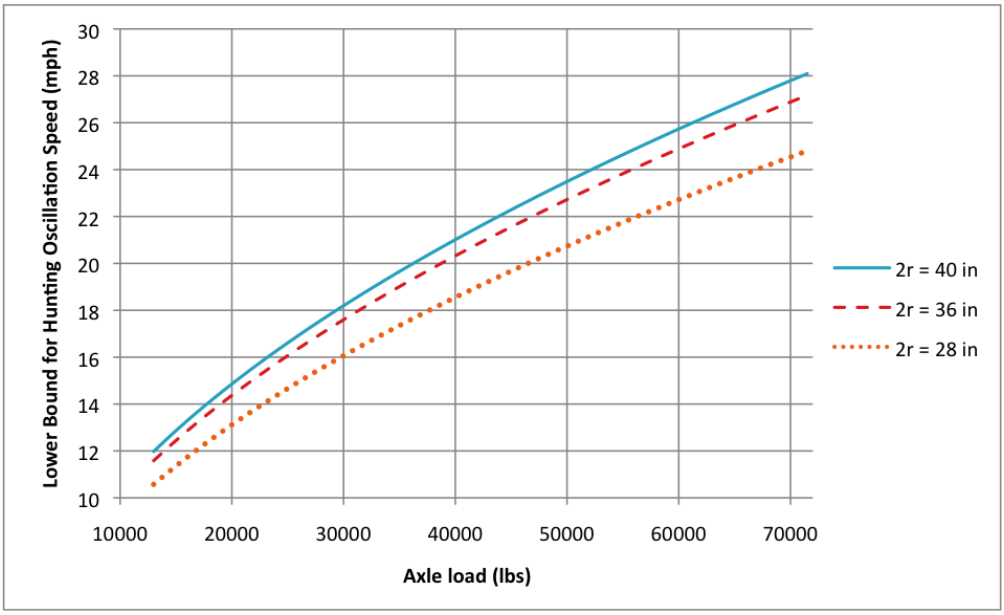

Rail Gauge

The United States and much of the world maintain their track at a standard gauge of 56.5 inches. US industrial standards often allow no more than an inch of deviation before lowering the track classification and requiring lower speeds until repairs. Other gauge systems exist throughout the world, such as the narrow meter gauge (39.4 in) in south Asia and the 66.0-inch broad gauge in India. In general, narrow gauge decreases and wider gauge increases both the upper and lower limit on the maximum safe speed before hunting oscillation (see Figures 4.8 and 4.9).

Figure 4.8: Upper bound on the critical speed of hunting oscillation as a function of axle load for a wheel ($r = 18$ in) on different world gauges.

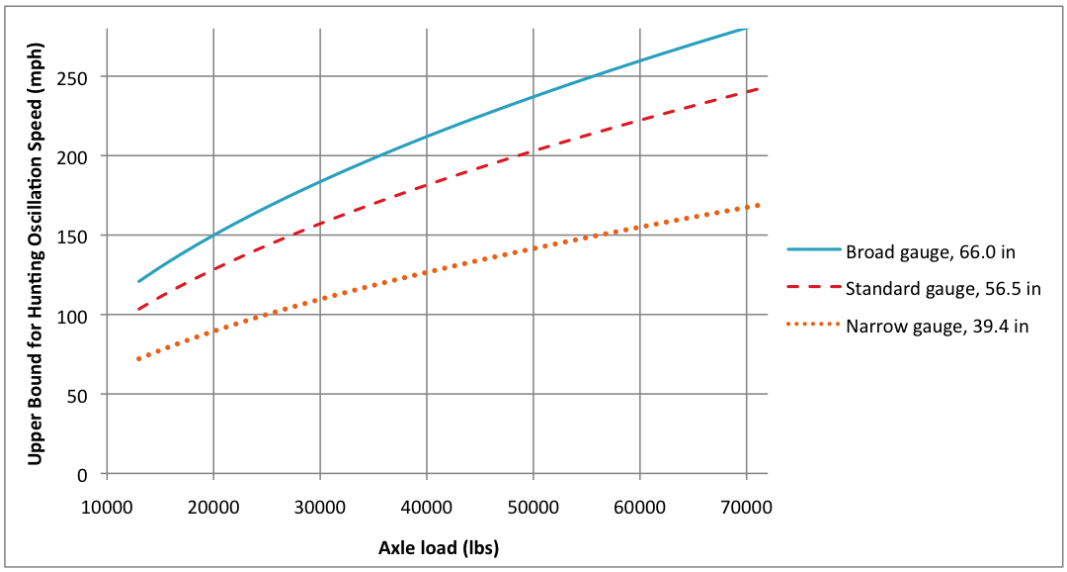

Figure 4.9: Lower bound on the critical speed of hunting oscillation as a function of axle load for a wheel ($r = 18$ in) on different world gauges.

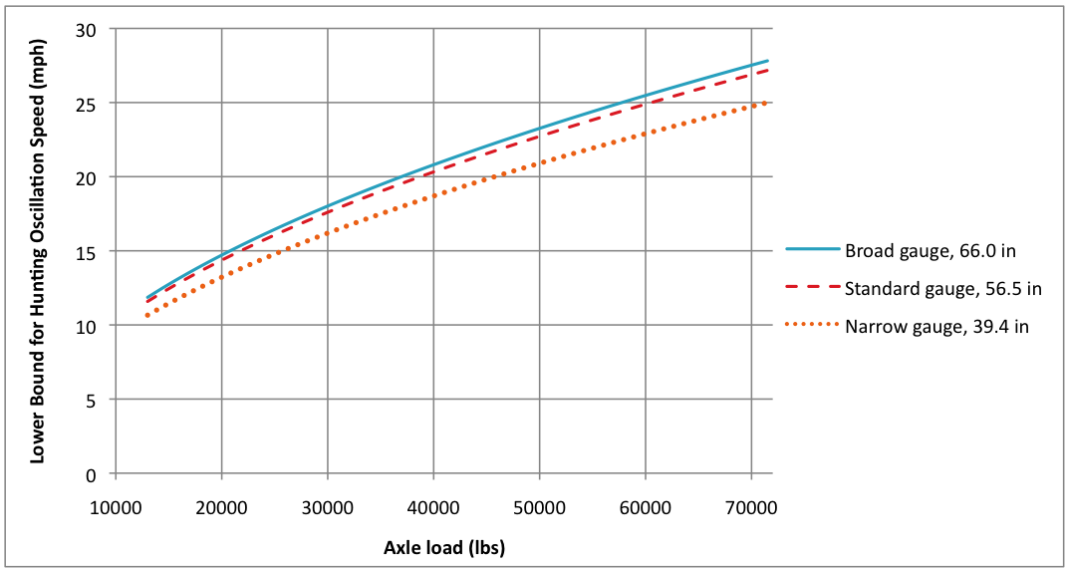

4.3.2 Oscillation Angle and Coning

The upper limit of the critical speed of hunting oscillation was derived from approximations of inertial and frictional forces and therefore takes into account the axle yaw, θ, and the wheel

tread conicity, *alpha*. Therefore, this equation can account for changes in the periodic motion of the wheelset, particularly those induced by severe wheel wear [1]. We have already shown that as wheels wear over time, flange thickness decreases and effective conicity increases, contributing to oscillations of higher frequency and amplitude in both lateral displacement and yaw. We have shown that a new wheel has a conicity of 0.05 and a maximum axle yaw of 2 degrees, while a worn wheel has a conicity of 0.35 and a maximum yaw of 6 degrees. Figure 4.10 shows the upper bound for the critical speed of the onset of hunting oscillation as a function of axle load in pounds for a new and a worn-out wheel. We can see that for any railcar weight, the speed at which hunting instability occurs is drastically reduced for worn wheels compared to new ones. So not only does wear of the wheel profile affect the amplitude and periodicity of the oscillation, but also causes oscillation at much lower operating speeds.

Figure 4.10: Upper bound on the critical speed of hunting oscillation as a function of axle load for new and worn wheels ($r = 18$ in).

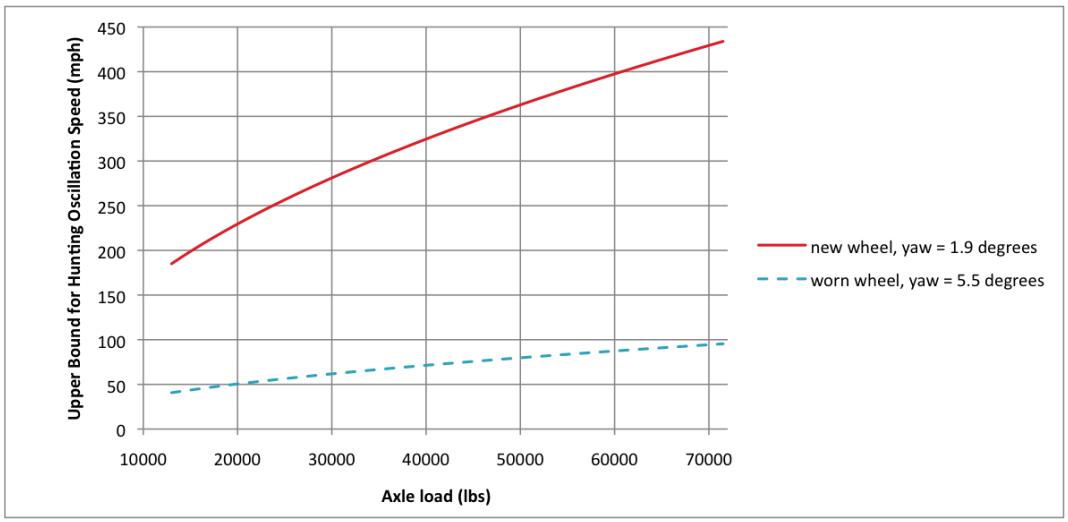

New wheels give upper bounds for hunting instability that are not restrictive for even the fastest passenger travel (125 mph) in the United States. But when considering speed limits for straight sections of track, railroad companies must consider all of the trains and wheelsets in service. This means that companies are often forced to balance increased speed, yielding more efficient traffic flow and revenue, and costly maintenance regiments. Often the cost of re-profiling or buying new wheels may be more expensive than the money lost from lower speeds.

[1] If the wear profile is known, the more refined Equation (3.16) derived from energy considerations in [25] can be used to show the affects of wheel wear on the lower bound of the critical speed.

4.4 Best Practices for Straight Track Design

Truck hunting refers to the oscillatory yawing of the vehicle trucks between the rails. Truck hunting increases lateral wheel-rail forces and can result in derailment by wheel climb and other instabilities. Therefore a major concern of tangent track construction is the operating speed at which wheelset oscillations remain damped out. In practice, truck hunting generally involves empty or lightly loaded cars, train speeds above 45 mph, dry rail, tangent or near-tangent track, roller bearing wheel sets, worn wheel treads, and good quality track [16].

We have shown that the periodic motion (in lateral displacement and axle yaw) of truck hunting is more pronounced, in both amplitude and frequency, when there is greater standard play between the wheelset and the rails. In other words, hunting oscillation is more violent when the track gauge is significantly wider than the wheel gauge, or axle width. This greater standard play can often be attributed to wheel wear that reduces flange thickness or to defects in track alignment leading to wider gauge. Both of these factors can be reduced with more stringent maintenance and enforcement of tolerance limits. However, re-profiling wheelsets and replacing rail that has widened beyond tolerance limits are both expensive and disruptive to the rail system. Therefore, many railroad companies must balance the gains in safety from constant maintenance and minor repairs with maintaining profits and delivery schedules.

Maximum safe operating speeds on tangent sections of track are dictated by the critical speed of the onset of these hunting oscillations. The most important factor for this critical speed is the value of the axle load, or weight from the railcar on each individual wheelset. The heavier the car, the faster it can go before hunting instabilities occur. This means that faster, lighter passenger cars and empty freight cars are the most likely to exhibit hunting and potentially derail. This re-emphasizes the importance of managing the distribution of cars in freight trains (and passenger trains to a lesser extent).

Unlike with curved track, for which rail managers and engineers can vary curve radius and cant angle to increase maximum operating speeds, maximum stable speeds on straight track are less dependent on the strict geometries of the railcar, wheelset, and track. Therefore the kinematic approach to wheelset and railcar dynamics on straight track reveals fewer tips for increasing traffic flow. This is because the derivations presented do not consider the wheelset as a part of an overall truck and suspension system, which has been designed to help damp out these oscillations and allow faster speeds. What this kinematic approach does reveal, however, is the importance of industrial management and strict maintenance schedules.

Conclusion

Railroad systems throughout the world are facing pressures to increase efficiency and traffic flow. In the United States, this desire to increase the speed and number of trains on existing track is complicated by a number of factors, including the age of existing infrastructure, the inability to expand rail lines into nearby real estate, and the lack of lines dedicated to only passenger or only freight traffic. This work has attempted to consider these challenges in the context of the physical constraints inherent in the train-track system and to offer insight into how the US can optimize their existing network while maintaining their reputation of safety.

This thesis presents critical speed derivations and kinematic descriptions of motions and instabilities on curved and straight track using fundamental physical principles. Chapter 1 derived the maximum safe speed before overturning on a flat or superelevated curve and discussed other possible single-wheelset or slack-action derailments. Chapter 3 presented the periodic motion equations of a hunting wheelset in lateral displacement and axle yaw and derived an upper and lower bound on the critical speed of the onset of these unstable hunting oscillations. The equations derived in Chapters 1 and 3 are not meant to be accurate predictors of speed limits on these respective sections of track; instead, they are meant to show how the critical speed of a railcar or wheelset depends on certain geometric factors.

Chapters 2 and 4 presented my analysis of the parameters that affect these maximum safe operating speeds on curved and straight track respectively. In this way, I demonstrated how basic kinematics could illustrate some of the problems faced by railroad managers and engineers optimizing both curved and straight sections of level track. In particular, it is clear that the optimal track design depends on the character of the traffic along the route. Optimizing corridors shared by both freight and passenger rail is difficult because slower, heavier, and longer freight trains exhibit different dynamics than faster, lighter, and shorter passenger trains. I showed that heavy, slow freight trains often have more trouble in curving situations while hunting oscillations on straight track are more likely to present a problem for lighter, faster passenger cars.

For curved track, I showed that the best practice for increasing speed for all traffic was

to make the curve gentler (increase the radius). This approach allowed passenger trains to traverse the curve more quickly without adversely affecting the slower, heavier freight traffic. In fact, gentler curves could also help to reduce slack-related derailments such as jackknifing or stringlining in long freight trains. I also discussed why the rail industry often uses the easier and cheaper approach of banking curves and how this can present problems for the slowest, top-heavy freight trains as it introduces a minimum curving speed. This minimum speed for freight traffic also illustrated the importance of loading and distribution of cars within the train. Taking these into account, I concluded that coupling empty cars only at the very rear of the train was the best case for curving stability, but that this could be costly in time and labor and thus is not always a profit-maximizing business practice.

In comparison to curved track, it is clear that on straight track the geometries of the track, wheelset, and railcar cannot be manipulated as freely to reduce instabilities. Instead, oscillations must often be counteracted with suspension systems that are not included in the first-order kinematic approximation and therefore beyond the scope of this work. Therefore, this analysis yields fewer suggestions for safely increasing the maximum speed on tangent track. However, it does illustrate the importance of strict management and maintenance of rail and rolling stock. It is clear that track irregularities, such as gauge widening, can cause more forceful oscillations while wear on the wheelset during service can increase the frequency and amplitude of hunting oscillation as well as decrease the critical speed at which these instabilities occur. Therefore, understanding the dynamics of a railcar and wheelset on straight track does reinforce the lesson that scheduling and paying for regular maintenance, although sometimes disruptive to delivery of goods or passengers, is one of the best ways to prevent dangerous and even more costly derailments in the future.

Appendix A

Basic Geometry of the Wheelset

Each railroad wheelset consists of two steel wheels fixed to a common axle, so that each wheel rotates with a common angular velocity and there is a constant distance between the two wheels. Each wheel is flanged to provide guidance along the rail. The wheel treads are slightly coned to reduce the rubbing of the flange on the rail and to ease the motion of the vehicle on curves. The fixed axle, flange, and coned tread all contribute to the behavior of the rail and wheelset as a dynamical system.

Alignment of a basic railway wheelset on straight track.

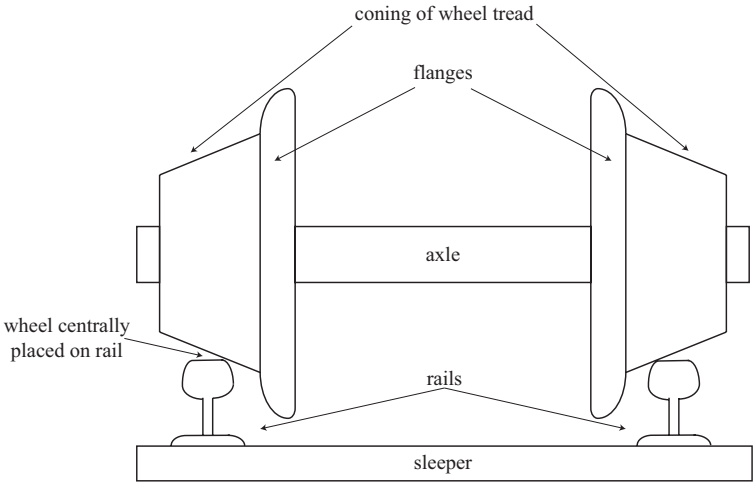

Coning

It is not known when the coning of the wheel treads was first introduced, but it was a well-established practice by the early 1820s. Nowadays wheel treads are manufactured with a taper or conicity, α, of 1/20 (or 1/40 for higher speed lines). This conicity is defined

as the slope of the tread in the horizontal direction perpendicular to the track. Coning is instrumental in the behavior and stability of the wheelset on both curved and straight track.

Flanges

The main function of the flange is the prevention of derailment, especially on sharp curves, switches, or crossings. Flanged rail wheels existed as early as the 17th century, however it was not until the 1820s when the location and play of the flange with respect to the rail began to be standardized. Initially there was debate over whether the flange should be positioned on the inside, outside, or even both sides of the wheel and there was little to no play allowed between the wheel flange and rail so that trains ran with constant flange-rail contact [7]. In the early 1830s flangeway clearance opened to reduce lateral forces between wheel and rail so that nowadays there is a lateral clearance, or play, of about $7 - 10$ mm. It is now also well established that flanges should be located on the inside of the wheel tread and rail to increase stability on both curved and straight track.

Alignment of a basic railway wheelset on curved track.

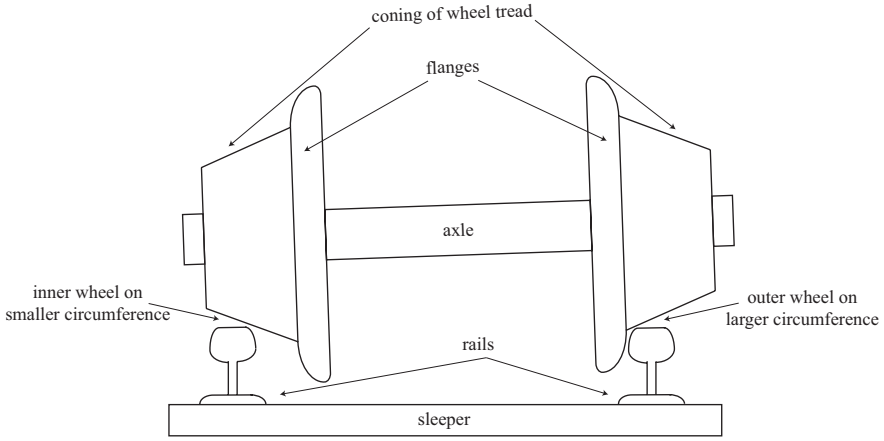

Appendix B

Wheelset Moment of Inertia Approximations

The moment of inertia of a composite body is equal to the sum of the moments of its individual pieces, so we can consider the moments of inertia of the axle and wheels separately and then sum them according to: $I_{wheelset} = I_{axle} + 2I_{wheel}$. We will approximate the moment of inertia of each of the wheels (ignoring the geometries of the flange and coning) and the axle as solid cylinders with specified radii and widths.

First we consider the moment of inertia about an the axis parallel to the width of the wheels and axle through the center of mass of the wheelset, $I_{||}$. This moment of inertia is used in the calculation of the rotational kinetic energy of the wheelset as it rolls forward along the track.

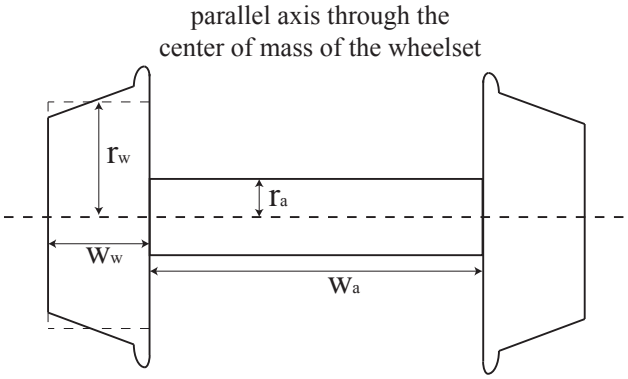

Due to inherent symmetry, we know that the moment of inertia of each of the two wheels will be the same. Since each wheel has a mass m_w and a radius r_w, the moment of inertia of a wheel is given by

$$I_{wheel} \approx \frac{1}{2} m_w r_w^2$$

Similarly, for the axle of mass m_a and smaller radius r_a, the moment of inertia is

$$I_{axle} \approx \frac{1}{2} m_a r_a^2$$

Therefore the total moment of inertia of the wheelset is given by the sum

$$I_{||} \approx \frac{1}{2} \left[m_a r_a^2 \right] + m_w r_w^2$$

Next we consider the moment of inertia about the perpendicular axis through the center of mass of the wheelset, $I_{\perp}$. This moment of inertia is used in the expression for the inertial force resisting the yawing motion of the axle during hunting oscillation.

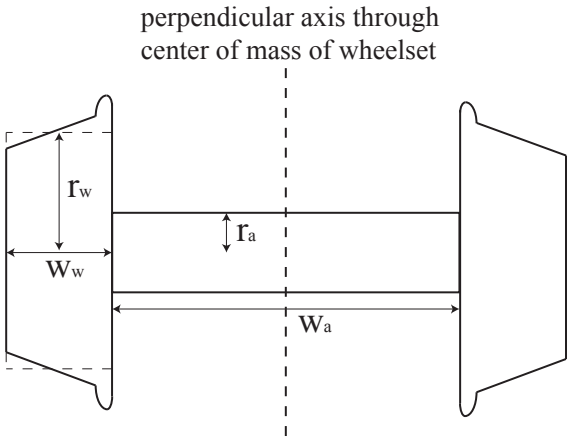

First we consider the moment of inertia of one of the wheels with mass m_w, radius r_w, and width w_w. Again symmetry dictates that the moment of inertia of each of the two wheels will be the same. The center of mass of each wheel is a distance $\frac{w_w}{2} + \frac{w_a}{2}$ from the axis of rotation, so we must use the parallel axis theorem. So approximating the moment of inertia of the wheel as the moment of inertia of a solid cylinder about a translated perpendicular axis, we get

$$I_{wheel} \approx \frac{1}{4} m_w r_w^2 + \frac{1}{3} m_w w_w^2 + m_w \left(\frac{1}{2} (w_w + w_a) \right)^2$$

Next we consider the moment of inertia for the axle of mass m_a, radius r_a, and width w_a. The perpendicular axis passes through the center of mass of the axle, so there is no translation term. So the moment of inertia is simply

$$I_{axle} \approx \frac{1}{4} m_a r_a^2 + \frac{1}{3} m_a w_a^2$$

So the total inertia of the wheelset is the sum of the moments of inertia of the two wheels

and the moment of inertia of the axle, so

$$I_{\perp} \approx \frac{1}{2}m_w r_w^2 + \frac{2}{3}m_w w_w^2 + \frac{1}{2}m_w \left(w_w + w_a\right)^2 + \frac{1}{4}m_a r_a^2 + \frac{1}{3}m_a w_a^2$$

For a North American standard freight wheel profile, AAR1B, we have the following values for the necessary geometries to find numerical approximations for a new wheelset on standard gauge:

- The weight of the wheelset is about 2200 lbs, with 900 lbs (27.973 slug) in each wheel and the remaining 400 lbs (12.432 slug) in the axle.
- The standard wheel has running radius of 18 inches (1.5 ft) and a tread width of 5.25 inches (0.4375 ft).
- The axle has a radius of approximately 5.5 inches (0.458 ft) and a length of 53.15 inches (4.429 ft)

With these values we find that the moment of inertia of the wheelset about an axis parallel to its length and through its center of mass is $I_{||} \approx 64$ slug $\cdot$ ft^2 and the moment of inertia of the wheelset about the perpendicular axis through its center of mass is $I_{\perp} \approx 448$ slug $\cdot$ ft^2.

Bibliography

[1] ISO 2631. *Mechanical vibration and shock - Evaluation of human exposure to whole-body vibration*. International Organization for Standards (ISO), 1997.

[2] ISO 3874/Amd 3:2005. *Double stack rail car operations*. International Organization for Standards (ISO), 1997.

[3] Circular No. 42-J. *General Rules Covering Loading of Carload Shipments of Commodities in Closed Cars*. Damage Prevention and Freight Claim Committee of the American Association of Railroads (AAR), January 2001. Available at `https://www.cn.ca/-/media/Files/Customer%20Centre/Shipping-Equipment/aar-rule5-circular-no42-j.pdf`.

[4] ISO 668. *Series 1 freight containers - Classification, dimensions and ratings*. International Organization for Standards (ISO), 2013.

[5] Mark Aldrich. *Death Rode the Rails: American Railroad Accidents and Safety, 1825-1965*. Johns Hopkins University Press, Baltimore, MD, 2006.

[6] American Railway Engineering and Maintenance-of-Way Association (AREMA), Lanham, MD. *Manual for Railway Engineering*, 2012.

[7] Jean-Bernard Ayasse and Hugues Chollet. Chapter 4: Wheel-rail contact. In Simon Iwnicki, editor, *Handbook of Railway Vehicle Dynamics*, pages 209–237. CRC Press, Taylor & Francis Group, Boca Raton, FL, 2006.

[8] George Bibel. *Train Wreck: The Forensics of Rail Disasters*. Johns Hopkins University Press, Baltimore, MD, 2012.

[9] Nicholas Faith. *Derail: Why Trains Crash*. Channel 4 Books (Macmillan Publishers Ltd), London, 2000.

[10] Gerald L. Foster. *A Field Guide to Trains of North America*. Houghton Mifflin, Boston, MA, 1996.

[11] Ken Harris and Jackie Tee. *IHS Jane's World Railways*. Janes Information Group, 54 edition, November 2012.

[12] George W. Hilton. A history of track gauge: How 4 ft 8-1/2 inches became the standard, May 1. Available at `http://trn.trains.com/sitecore/content/Home/Railroad%20Reference/Railroad%20History/2006/05/A%20history%20of%20track%20gauge.aspx?sc_lang=en`.

[13] Klingel. Uber den lauf der eisenbahnwagen auf gerarder bahn. volume 20, pages 113–123, Tafel XXI.

[14] C. Sujatha K.V. Gangadharan and V. Ramamurti. Experimental and analytical ride comfort evaluation of a railway coach, 2004. Available at `http://sem-proceedings.com/22i/sem.org-IMAC-XXII-Conf-s20p08-Experimental_Analytical-Ride-Comfort-Evaluation-Railway-Coach.pdf`.

[15] James R. Loumiet. Freight train slack action effects analysis. Nashville, TN, May 1996. Presented to National Association of Railroad Safety Consultants and Investigators.

[16] James R. Loumiet and William G. Jungbauer, editors. *Train Accident Reconstruction and FELA and Railroad Litigation*. Lawyers & Judges Publishing, Tucson, AZ, 5th edition, 2011.

[17] Dennis P. McIlnay. *The Wreck of the Red Arrow: An American Train Tragedy*. Seven Oaks Press, Hollidaysburg, PA, 2010.

[18] Silviu Nastac and Mihaela Picu. Evaluating methods of whole-body-vibration exposure in trains. *Annals of "Dunarea de Jos" University of Galati Fascicle XIV Mechanical Engineering*, pages 55–60, 2010. Available at `http://www.ann.ugal.ro/im/Anale%202010/Volumul_II/L10,%20C.pdf`.

[19] The Washington Post Online. All aboard amtrack's acela. Available at `http://www.washingtonpost.com/wp-srv/travel/features/acelaflash.htm`.

[20] World Trade Press Online. Guide to railcars. Available at `http://worldtraderef.com/WTR_site/Rail_Cars/Guide_to_Rail_Cars.asp`.

[21] Vassilios A. Profillidis. *Railway Management and Engineering*. Ashgate Publishing Ltd., Burlington, VT, 3 edition, 2006.

[22] BNSF Railways. Box car 50 ft. 286 grl. Available at `http://www.bnsf.com/customers/pdf/50ftF_BoxcarDiagram.pdf`.

[23] F.J. Redtenbacher. *Die Gasetze des Locomotiv-Baues*. Manheim: Verlag von F. Bassermann, 1855.

[24] The Telegraph. Double-decker trains may ease overcrowding, December 30 2005.

[25] A.H. Wickens. The dynamics of railway vehicles on straight track: Fundamental considerations of lateral stability. *Proc. Inst. Mech. Eng.*, pages 29–, 1965-66.

[26] A.H. Wickens. *Fundamentals of Rail Vehicle Dynamics: Guidance and Stability*. Swets & Zeitlinger, Lisse, Netherlands, 2003.

[27] Huimin Wu and Semih Kalay. Management of the wheel/rail contact interface in heavy-haul operations (part 1 of 2). *Interface: The Journal of Wheel/Rail Interaction*, October 2009. Available at `http://interfacejournal.com/?p=265`.

[28] Huimin Wu and Nicholas Wilson. Chapter 8: Railway vehicle derailment and prevention. In Simon Iwnicki, editor, *Handbook of Railway Vehicle Dynamics*, pages 209–237. CRC Press, Taylor & Francis Group, Boca Raton, FL, 2006.

[29] S.W. Kim C.K. Park Y.G. Kim, H.B. Kwon and T.W. Park. Correlation of ride comfort evaluation methods for railway vehicles. *Proceedings of the Institution of Mechanical Engineers Part F - Journal of Rail and Rapid Transit*, 217(2):73–88, 2003.